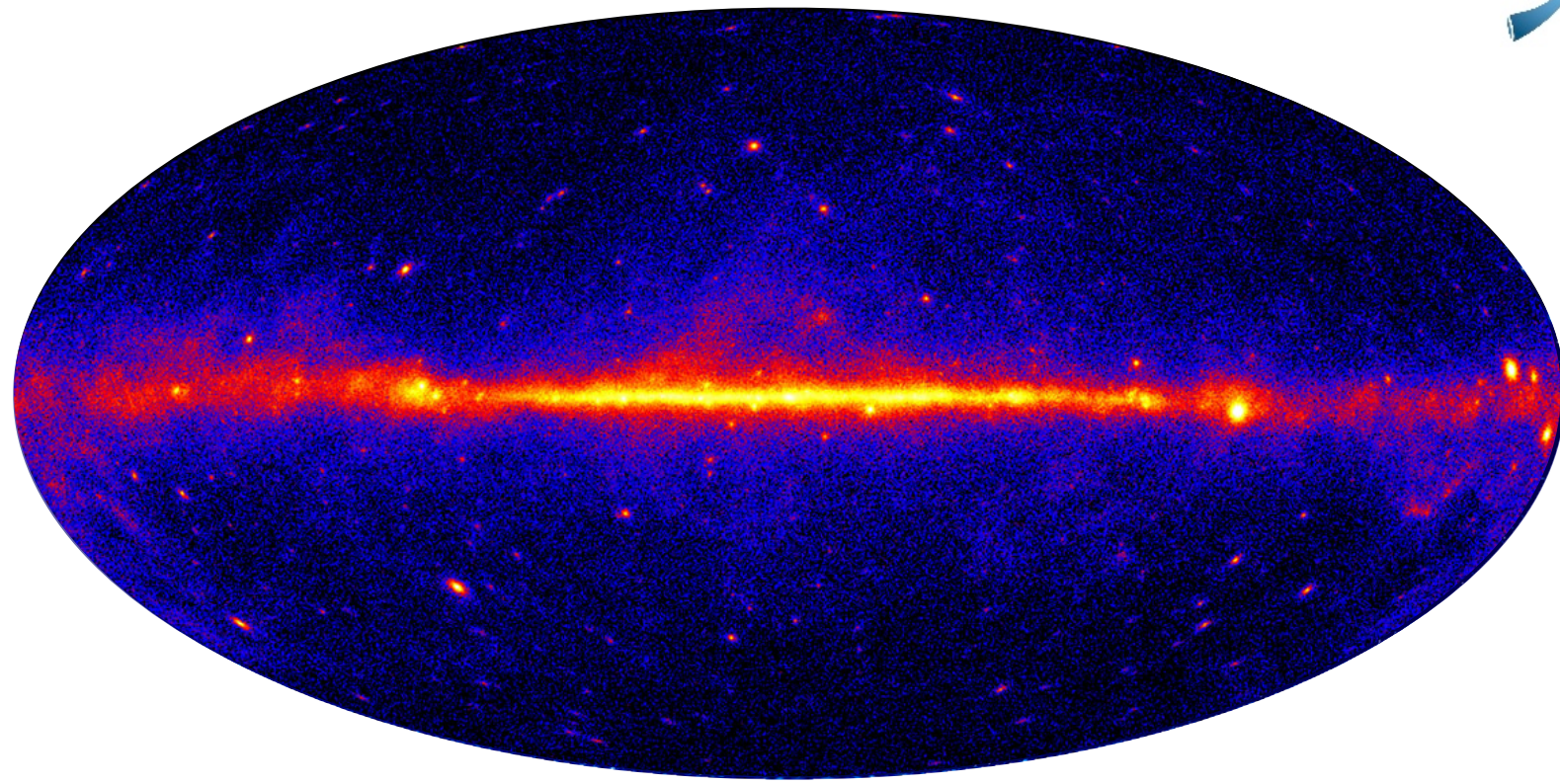




Recent advances and open issues in understanding the diffuse gamma-ray background

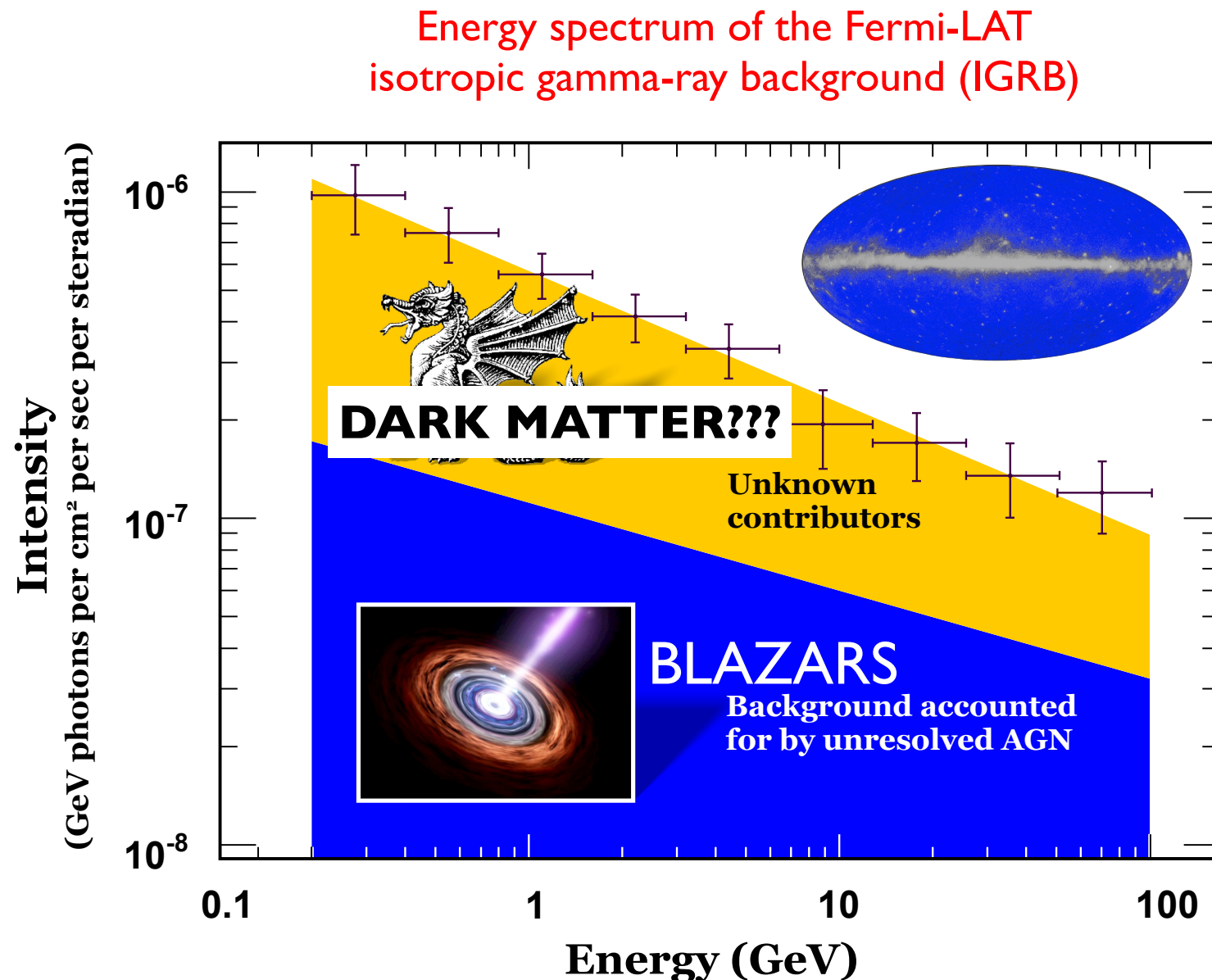
Jennifer Siegal-Gaskins
Caltech

Image Credit: NASA/DOE/International LAT Team



Jennifer Siegal-Gaskins
Caltech

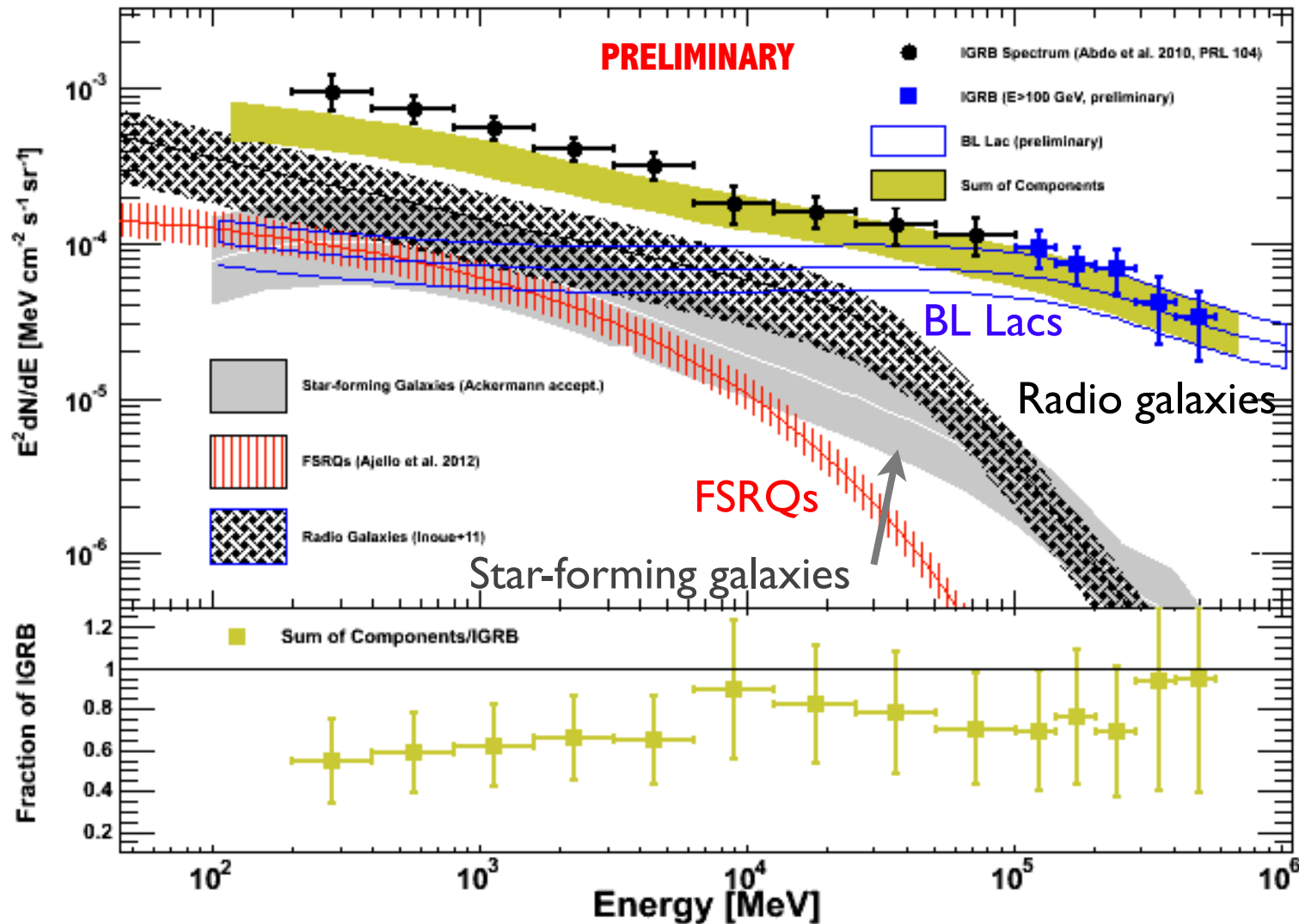
What is making the diffuse gamma-ray background?



Credit: NASA/DOE/Fermi LAT Collaboration

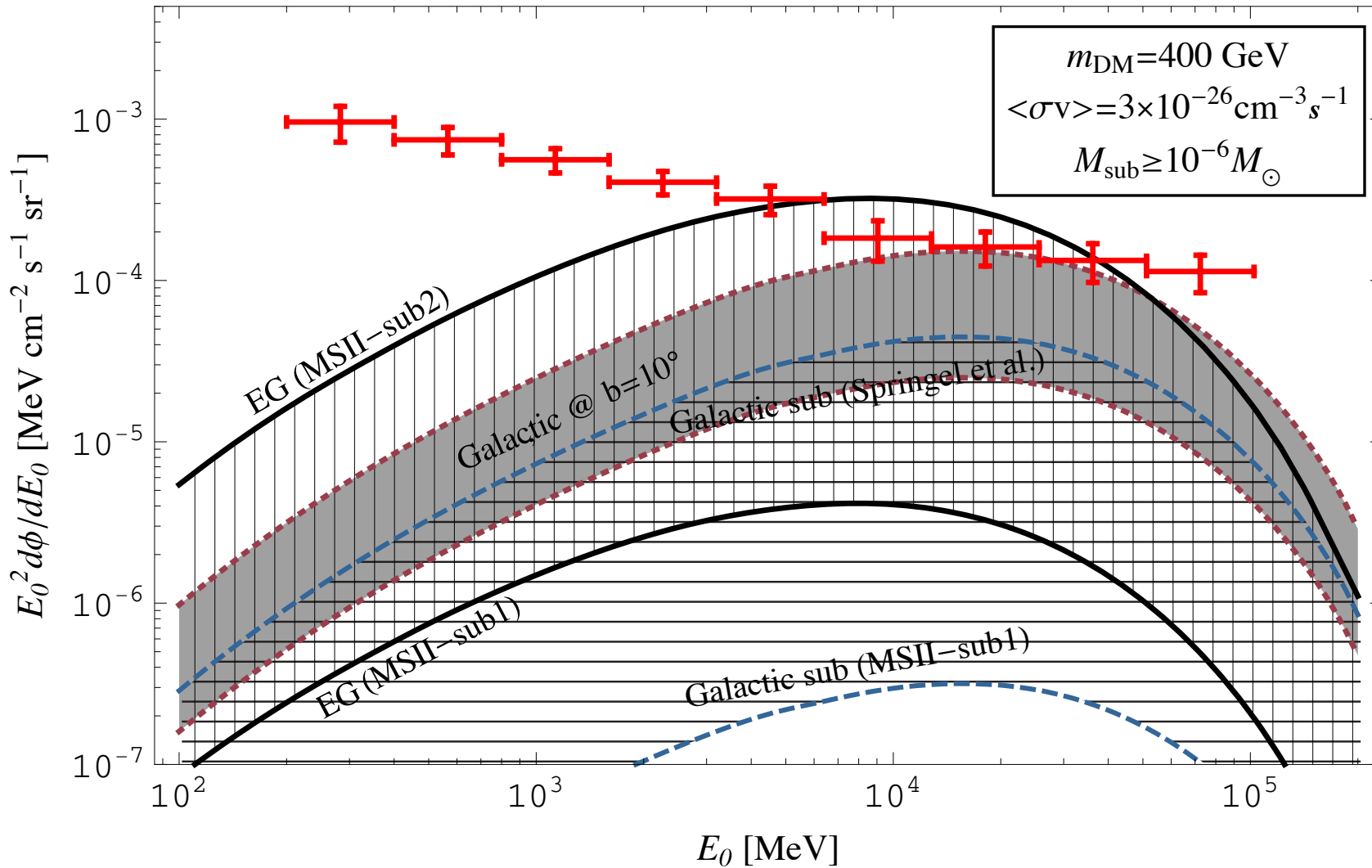
What is making the diffuse gamma-ray background?

Expected contribution of source populations to the IGRB



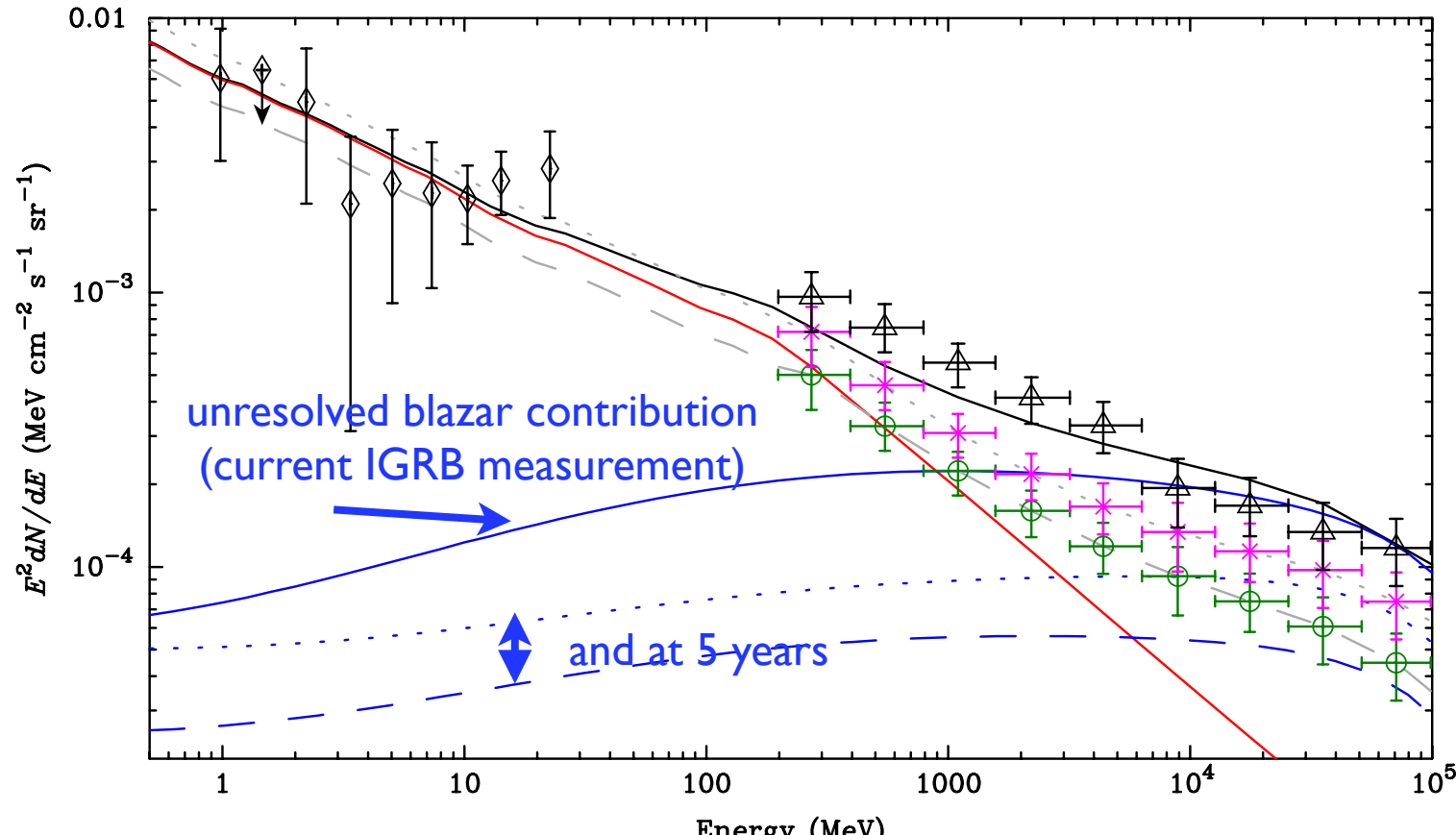
Sum is $\sim 60\text{-}100\%$ of IGRB intensity (energy-dependent)

Dark matter signals in the IGRB



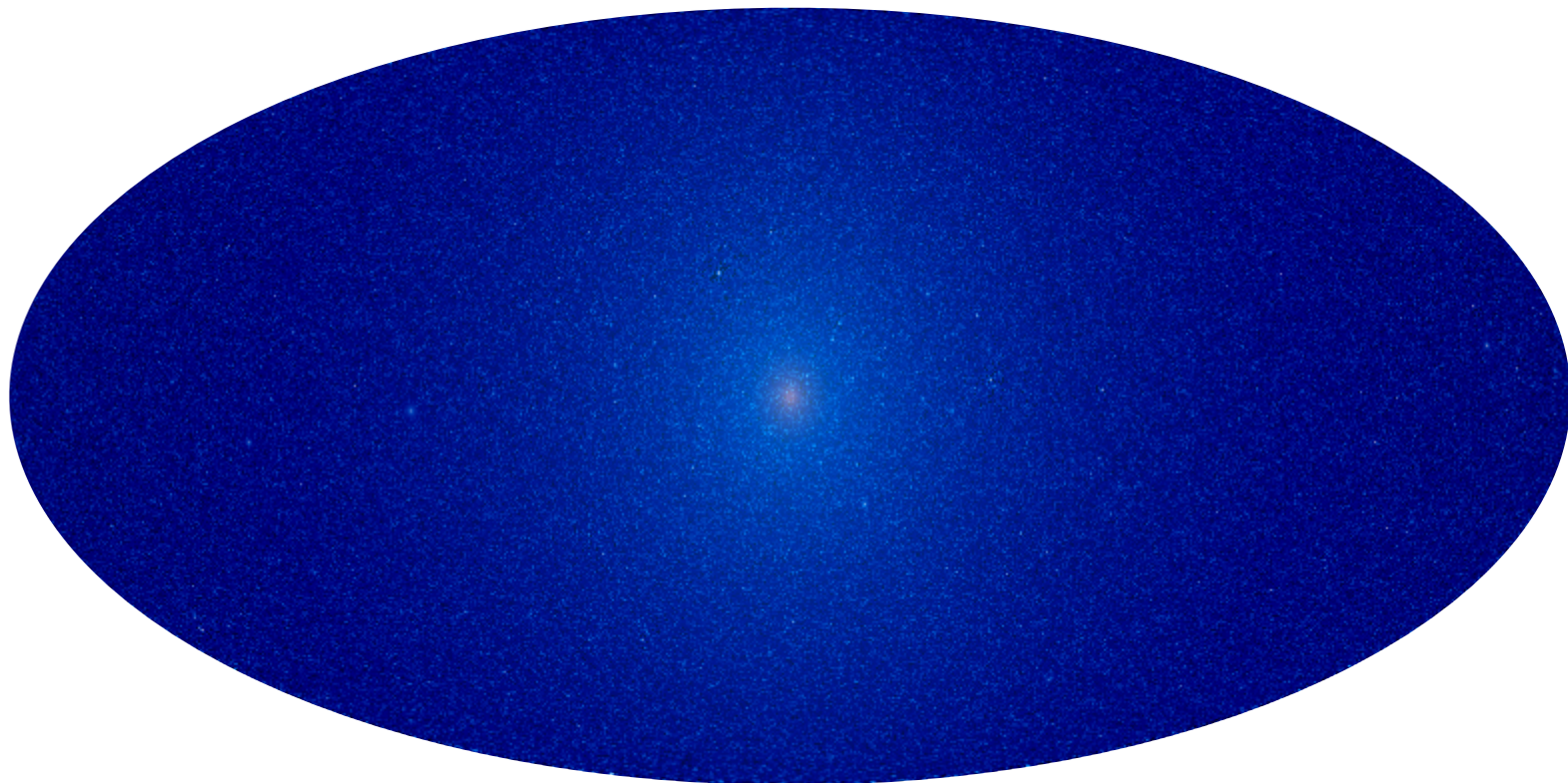
Abdo et al., JCAP 04 014 (2010)

Getting rid of the IGRB



- the IGRB is time-dependent: will get less intense as more sources are resolved
- understanding of unresolved source contributions will also improve
- future IGRB measurements will lead to improved DM sensitivity

Detecting unresolved sources with anisotropies



Diffuse emission that originates from one or more **unresolved source populations** will contain **fluctuations on small angular scales** due to variations in the number density of sources in different sky directions

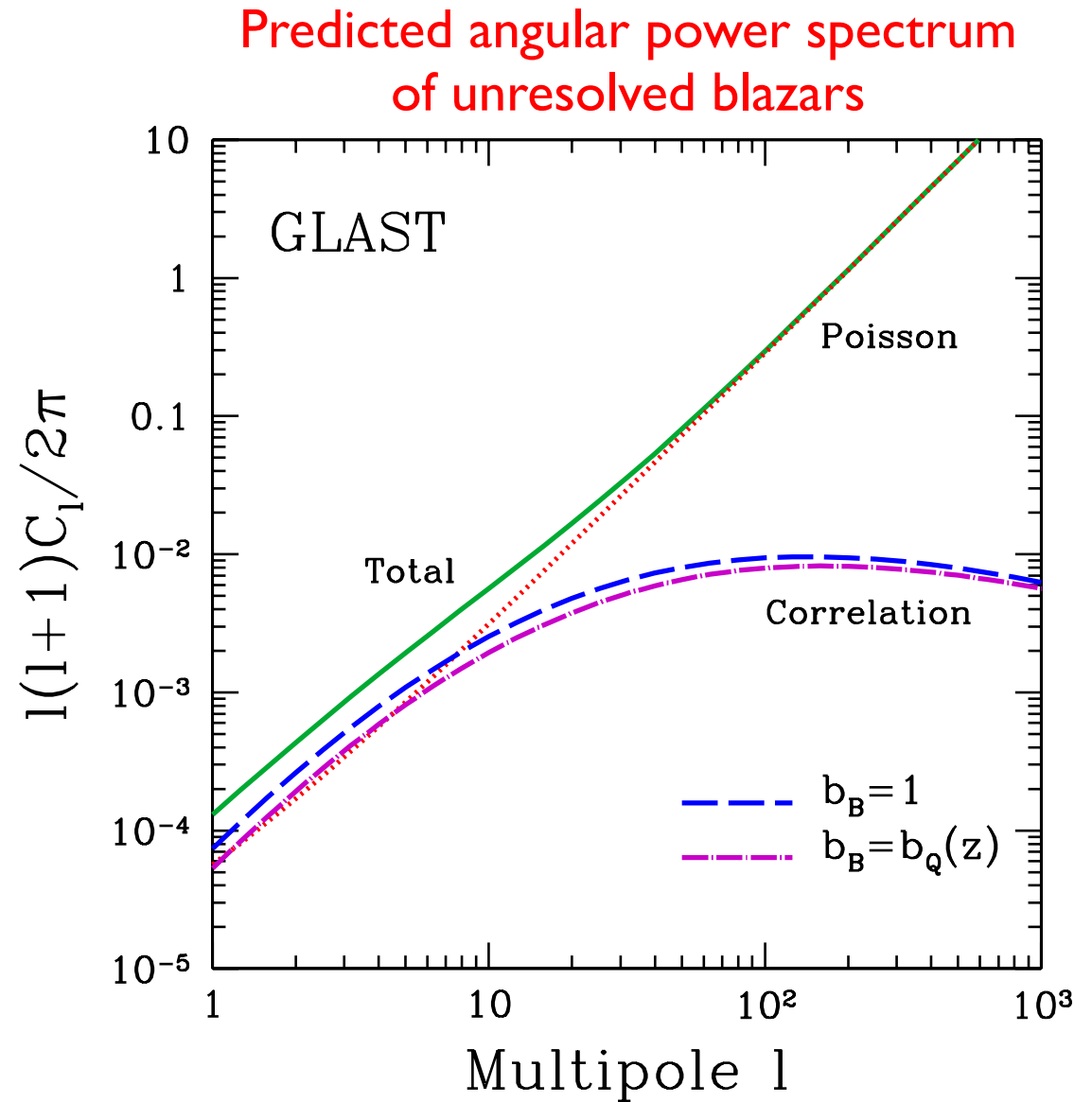
Anisotropy is another IGRB observable!!!

Angular power spectra of unresolved gamma-ray sources

- the angular power spectrum of many gamma-ray source classes (except dark matter) is dominated by the Poisson (shot noise) component for multipoles greater than ~ 10
- Poisson angular power arises from unclustered point sources and takes the same value at all multipoles

predicted fluctuation angular power $C_\ell/\langle I \rangle^2 [\text{sr}]$ at $\ell = 100$ for a single source class
(LARGE UNCERTAINTIES):

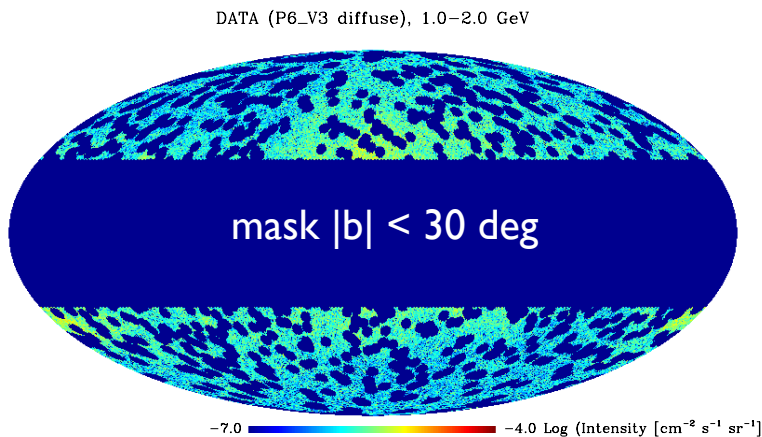
- blazars: $\sim 2\text{e-}4$
- starforming galaxies: $\sim 2\text{e-}7$
- dark matter: $\sim 1\text{e-}6$ to $\sim 1\text{e-}4$
- MSPs: ~ 0.03



Ando, Komatsu, Narumoto & Totani 2007

Fermi LAT anisotropy measurement

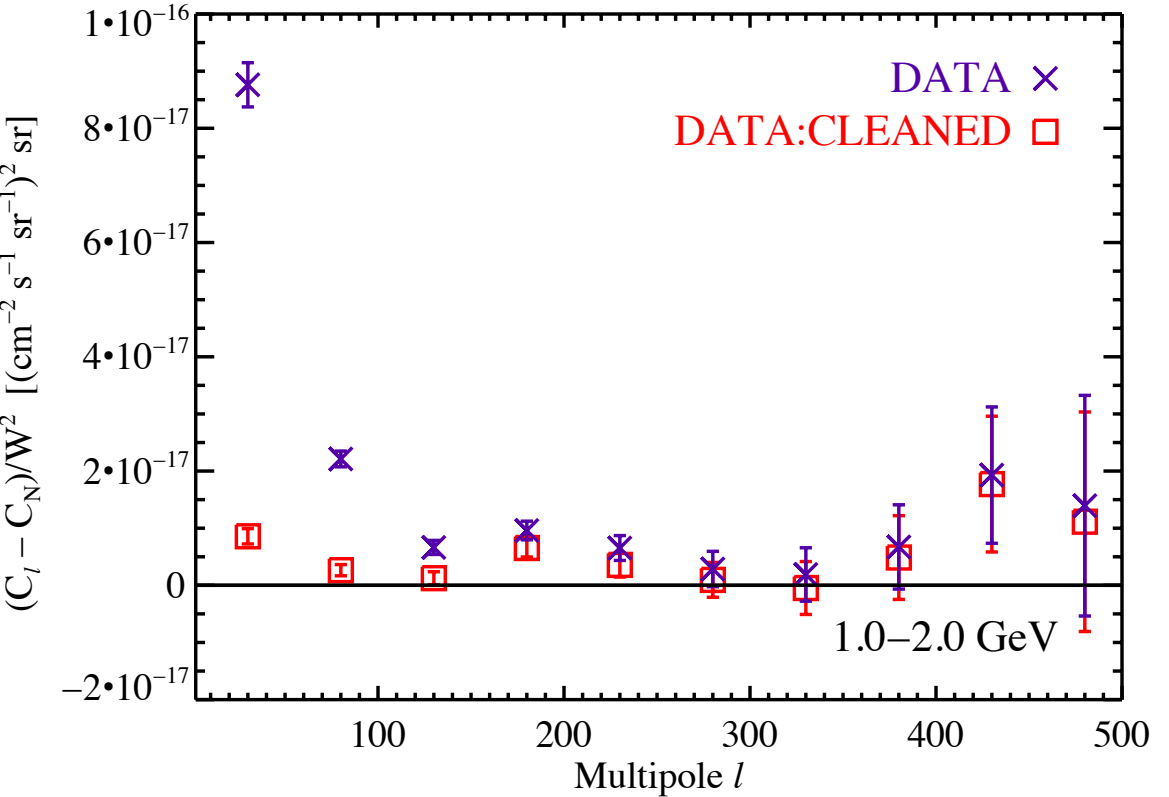
Map with default mask applied



- at $l \geq 155$, detected signal is consistent with Poisson angular power C_P (i.e., unclustered point sources)
- significant ($>3\sigma$) detection of angular power up to 10 GeV, lower significance power measured at 10-50 GeV
- small angular scale IGRB anisotropy measured for the first time with the Fermi LAT!

intensity angular power spectrum

DATA:CLEANED = DATA - Galactic diffuse model



Ackermann et al. [Fermi LAT Collaboration],
PRD 85, 083007 (2012)

Constraints from the fluctuation angular power

Constraints from best-fit constant fluctuation angular power ($\ell \geq 150$)
measured in the data and foreground-cleaned data

Source class	Predicted $C_{100}/\langle I \rangle^2$ [sr]	Maximum fraction of IGRB intensity	
		DATA	DATA:CLEANED
Blazars	2×10^{-4}	21%	19%
Star-forming galaxies	2×10^{-7}	100%	100%
Extragalactic dark matter annihilation	1×10^{-5}	95%	83%
Galactic dark matter annihilation	5×10^{-5}	43%	37%
Millisecond pulsars	3×10^{-2}	1.7%	1.5%

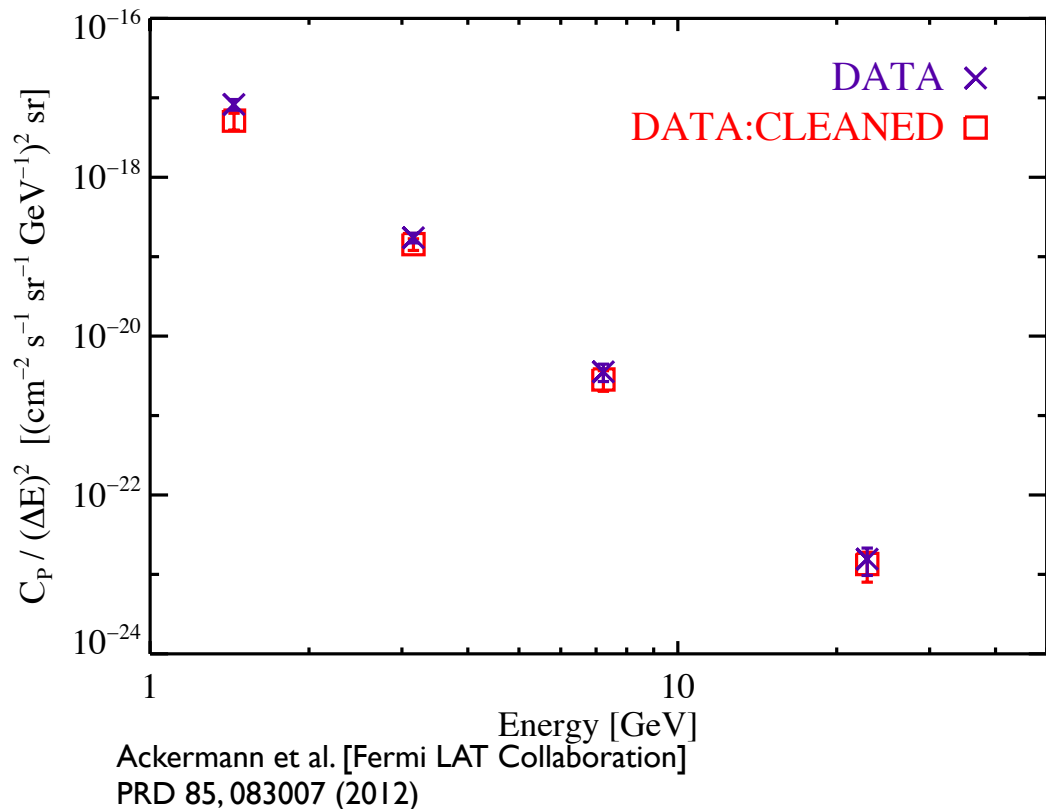
NB: these are indicative predicted values for source populations, taken from the literature.

- dependent on source model (large variations possible, especially for dark matter scenarios)
- dependent on source detection threshold
- for cosmological populations, dependent on EBL assumptions

These values may not be accurate for your favorite source population model.

Energy dependence of anisotropy

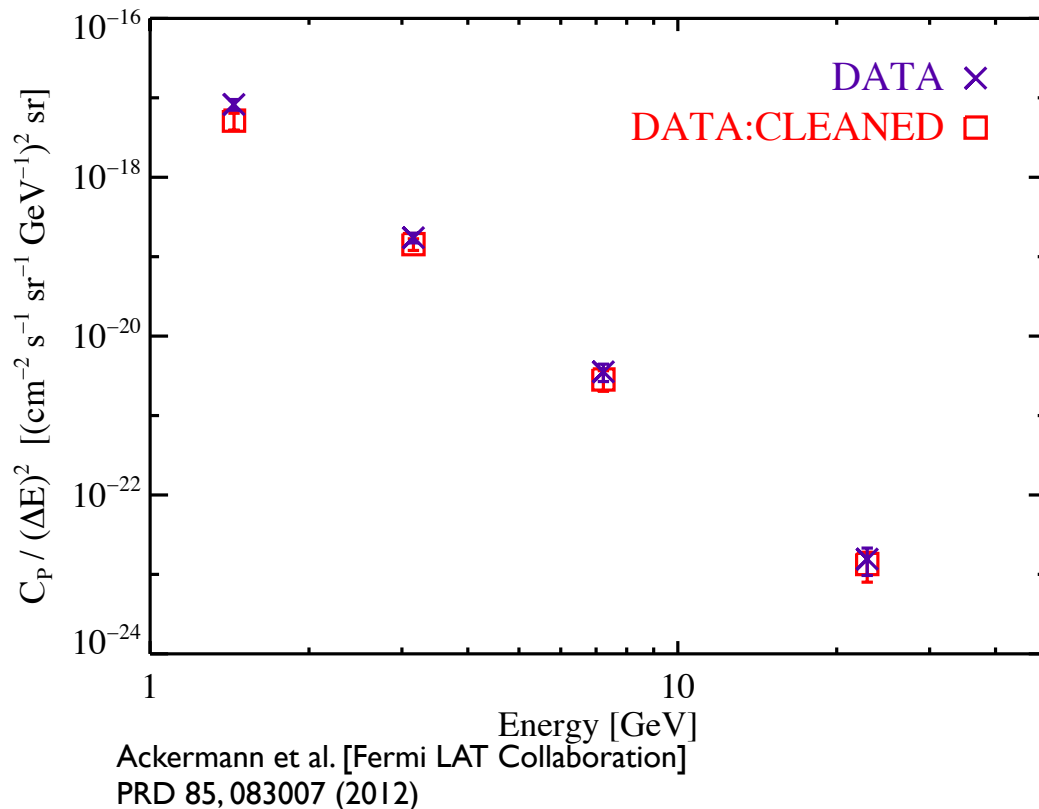
Intensity anisotropy energy spectrum



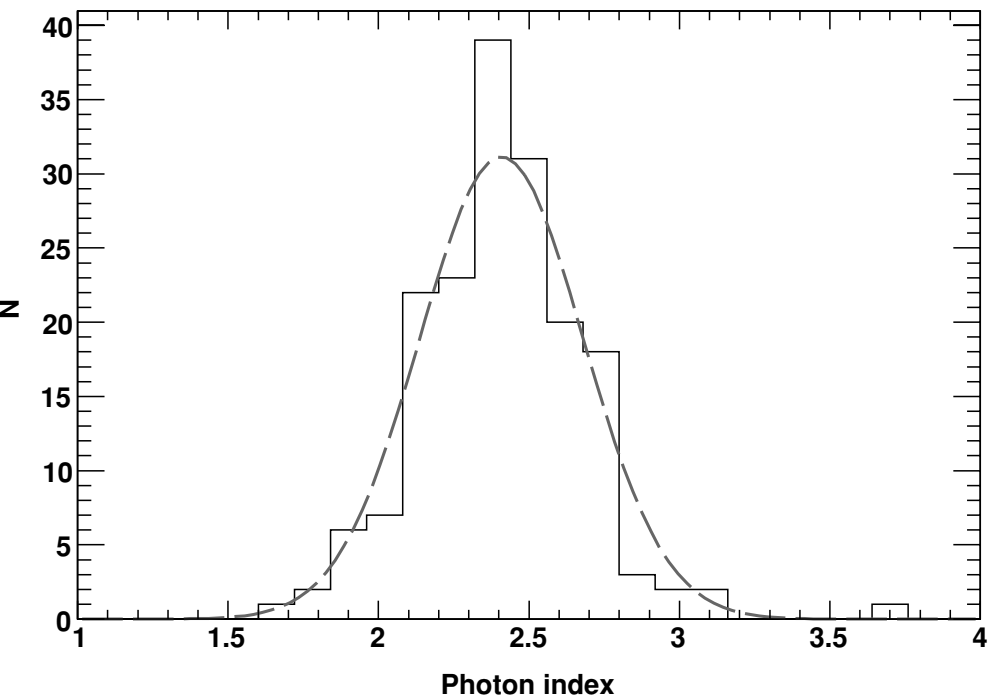
- consistent with a source class with power-law energy spectrum with $\Gamma = -2.40 \pm 0.07$ (- 2.33 ± 0.08 for cleaned data)

Energy dependence of anisotropy

Intensity anisotropy energy spectrum



Spectral indices of Fermi LAT sources

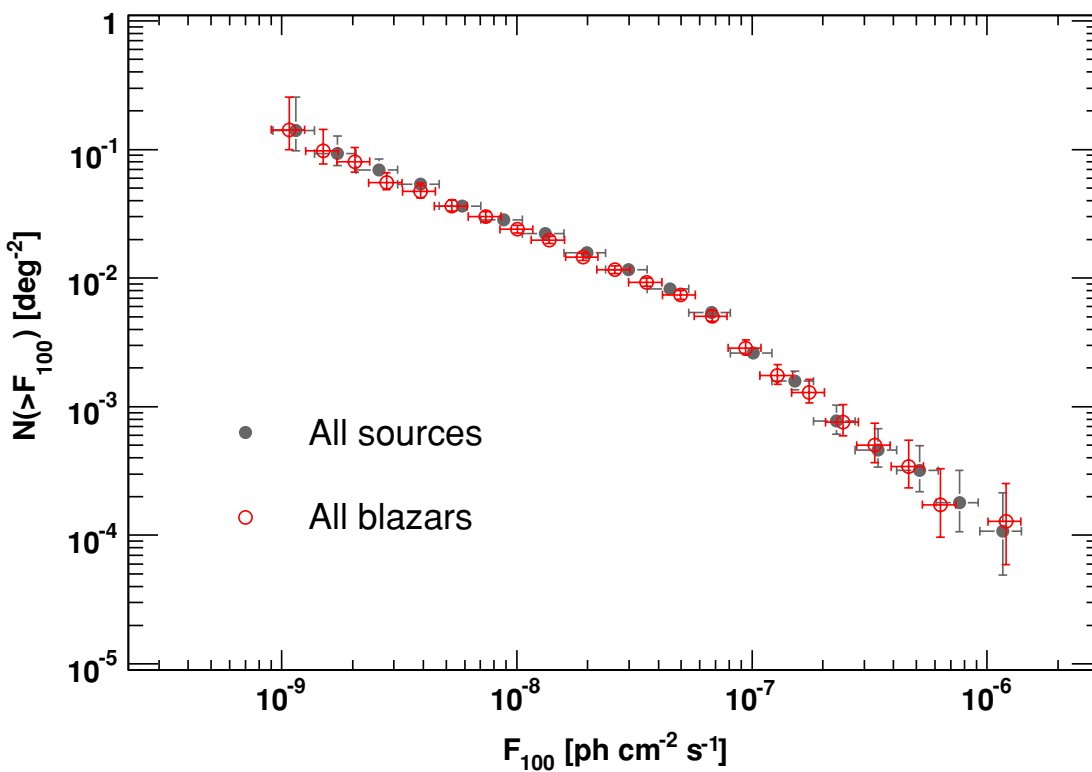


- consistent with a source class with power-law energy spectrum with $\Gamma = -2.40 \pm 0.07$ (-2.33 ± 0.08 for cleaned data)
- spectral index in good agreement with that of blazars

The source count distribution

the source count distribution (“LogN-LogS”) of Fermi-LAT–detected sources is consistent with a broken power law

LogN-LogS of Fermi LAT sources



Abdo et al. (Fermi LAT Collaboration), ApJ 720, 435 (2010)

high (bright-end)
spectral index

break flux

$\frac{dN}{dS} = \begin{cases} A S^{-\beta} & S \geq S_b \\ A S_b^{-\beta+\alpha} S^{-\alpha} & S < S_b \end{cases}$

low (faint-end)
spectral index

Anisotropy and source counts

the total intensity and Poisson angular power (C_P) from *unresolved* sources can be predicted from the source count distribution

$$I = \int_0^{S_t} \frac{dN}{dS} S dS \quad C_P = \int_0^{S_t} \frac{dN}{dS} S^2 dS$$

Anisotropy and source counts

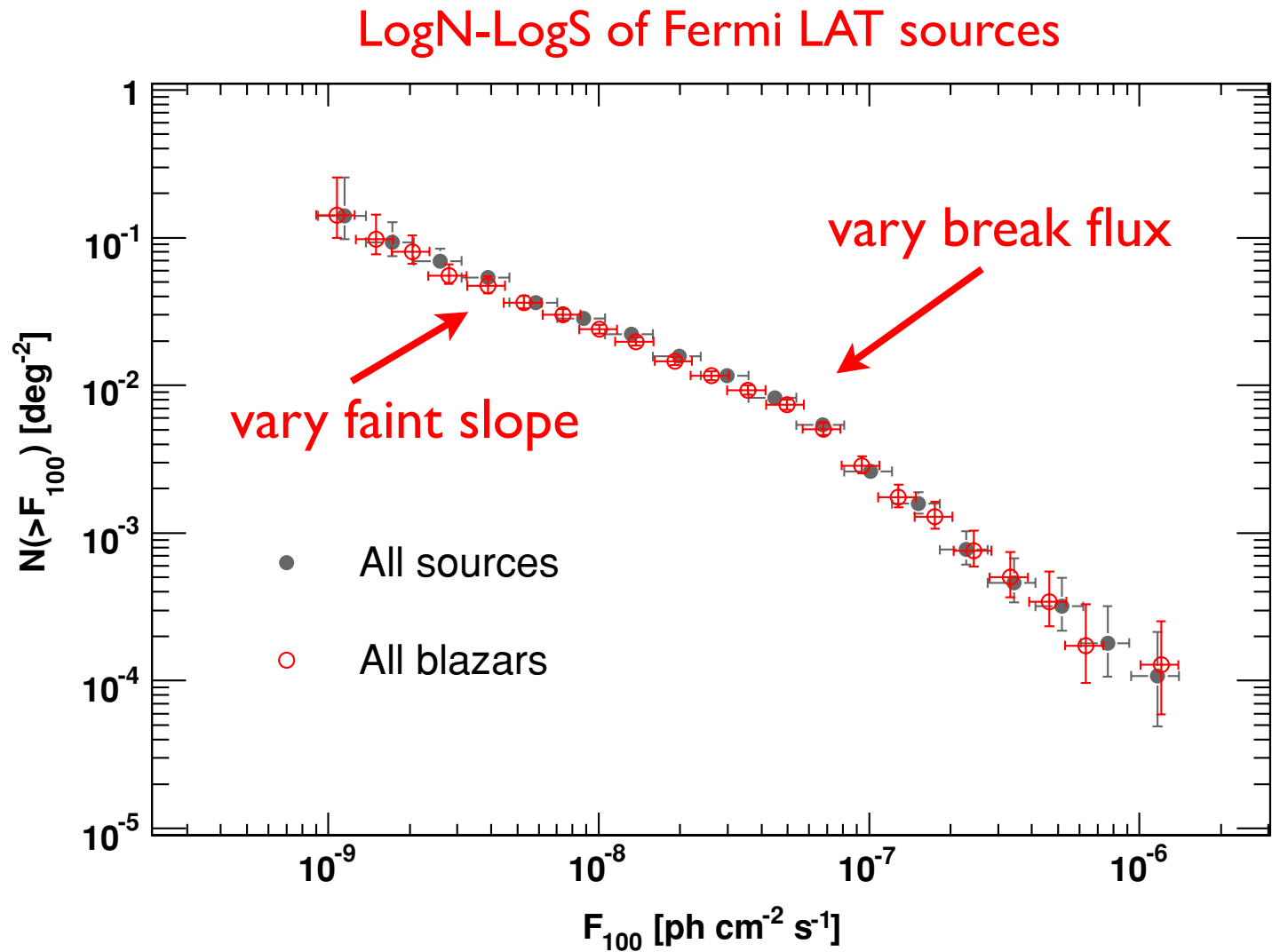
the total intensity and Poisson angular power (C_P) from *unresolved* sources can be predicted from the source count distribution

$$I = \int_0^{S_t} \frac{dN}{dS} S dS \quad C_P = \int_0^{S_t} \frac{dN}{dS} S^2 dS$$

How do the predicted intensity and angular power from unresolved blazars compare to the measured values?

Exploring the LogN-LogS parameter space

- we fix the high index and normalization of the source count distribution to the measured best-fit values
- we vary the low index and break flux, and calculate the intensity and anisotropy produced by the unresolved sources in the 1-10 GeV band

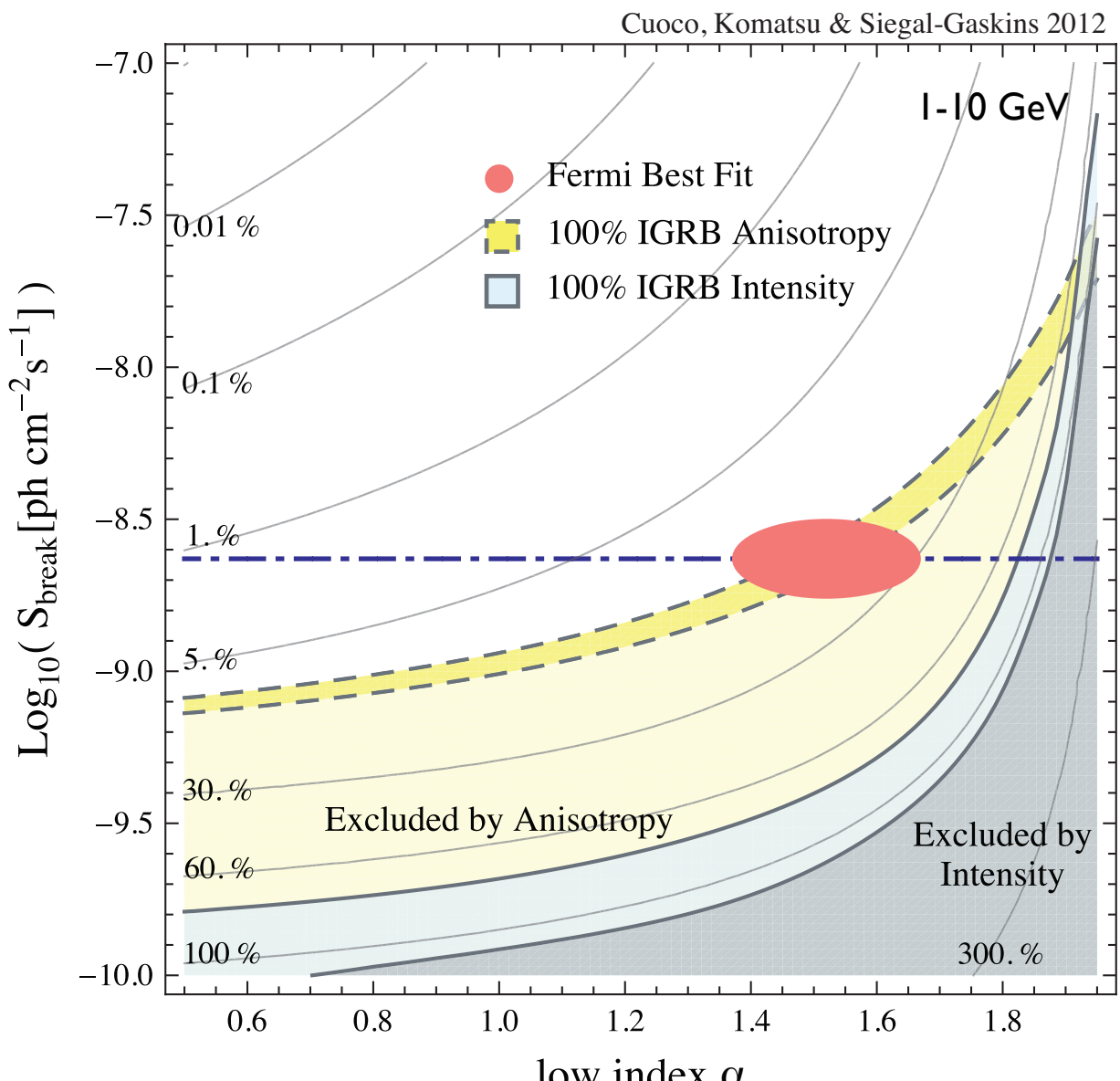


Abdo et al. [Fermi LAT Collaboration], ApJ 720, 435 (2010)

Constraints on unresolved gamma-ray sources

- anisotropy and source count analysis point to blazars contributing ~20% of IGRB intensity and ~100% of IGRB anisotropy
- this result implies that component(s) making ~80% of IGRB intensity have very low level of anisotropy
- anisotropy is a powerful constraint: measured angular power excludes Stecker & Venter 2011 model
- Harding & Abazajian 2012 find LDDE blazar model constrained to provide less than ~ 10% of IGRB intensity

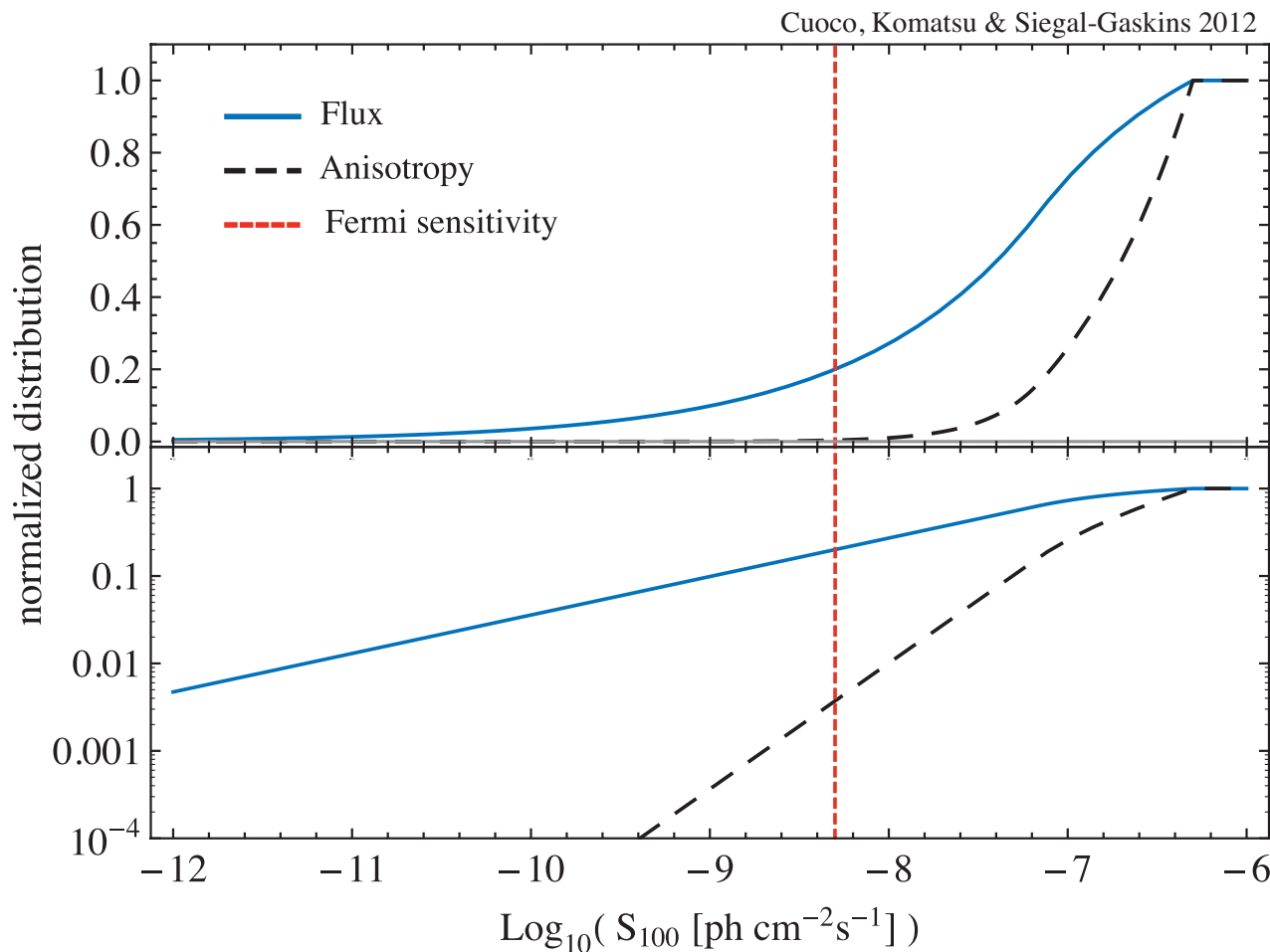
Constraints on source count distribution
(logN-logS) parameter space



Implications for blazar models

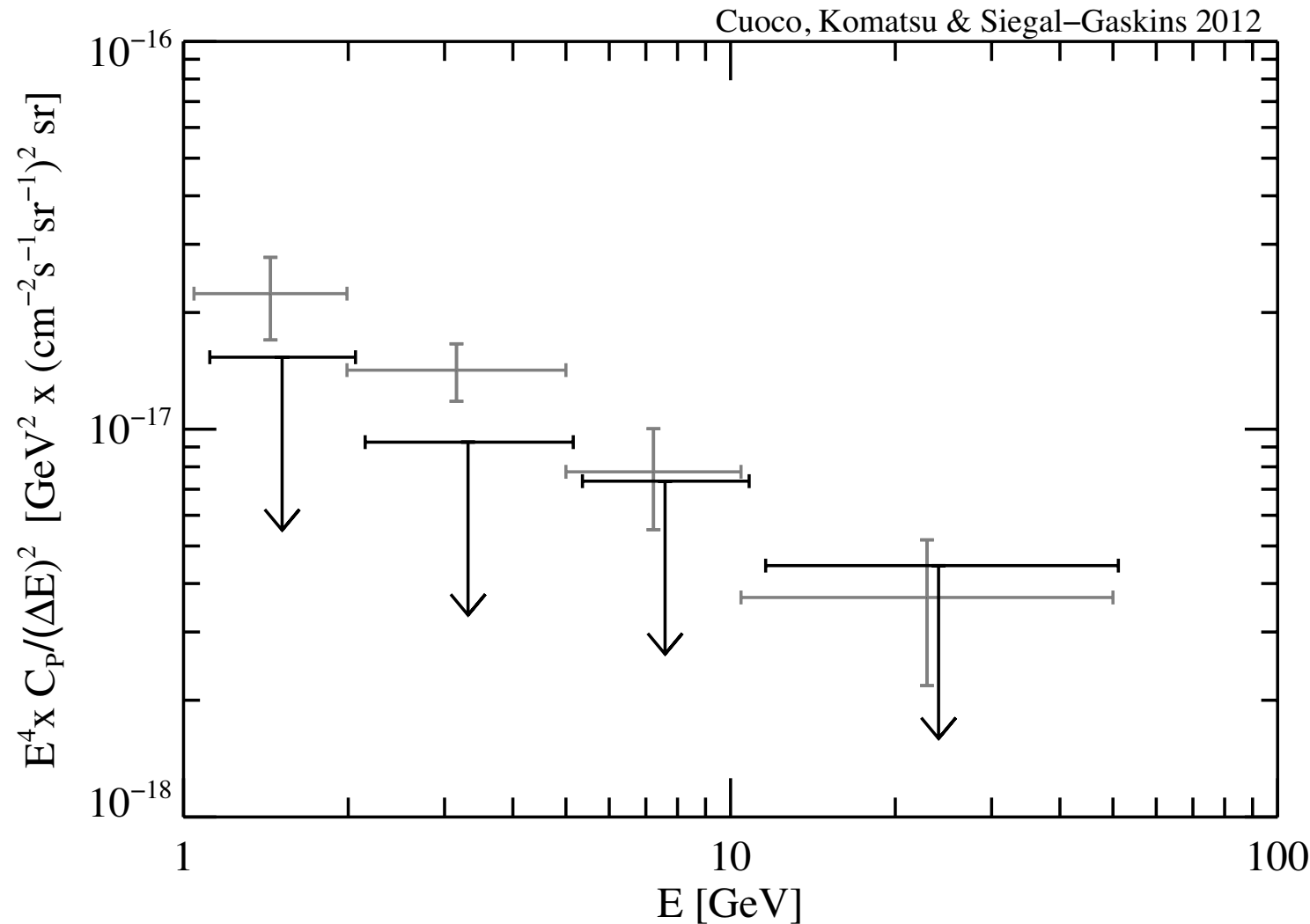
- anisotropy very sensitive to source count distribution just below detection threshold → difficult to construct a blazar model to avoid strong constraints
- as the source detection threshold decreases, the validity of predictions for the logN-logS of blazars (and other source populations) can be tested and revised

Cumulative flux and anisotropy contribution as a function of source flux $E > 100$ MeV



Constraints on IGRB anisotropy from non-blazar sources

Total measured angular power with 1-sigma uncertainties
and 2-sigma upper limits on non-blazar anisotropy



(calculated assuming blazar anisotropy given by best-fit source count parameters)

Summary

Recent advances:

- increase in detected sources has allowed improved estimates of IGRB contribution from known source populations
- IGRB small-scale anisotropy has been detected for the first time!
 - consistent with unclustered point sources
 - measured angular power constrains source populations
 - energy dependence is consistent with that of blazars
- source count analysis and anisotropy measurements point to blazars contributing ~100% of the anisotropy but only less than ~20% of the intensity of the IGRB

Open issues:

- what makes up the other ~80% of the IGRB intensity?
- how can we improve models of unresolved (known) source populations? / how much do we need to improve these to constrain possible new sources?
- how will the IGRB measured a few years from now change (in intensity and anisotropy) and what will that teach us about its origin?

Additional slides

The Fermi Large Area Telescope (LAT)

- launched in June 2008
- pair-production detector:
detects charged particles as
well as gamma rays
- excellent charged particle
event identification and
background rejection
- 20 MeV to > 300 GeV
- angular resolution ~ 0.1 deg
above 10 GeV
- uniform sky exposure of \sim
30 mins every 3 hrs

Fermi data is public!



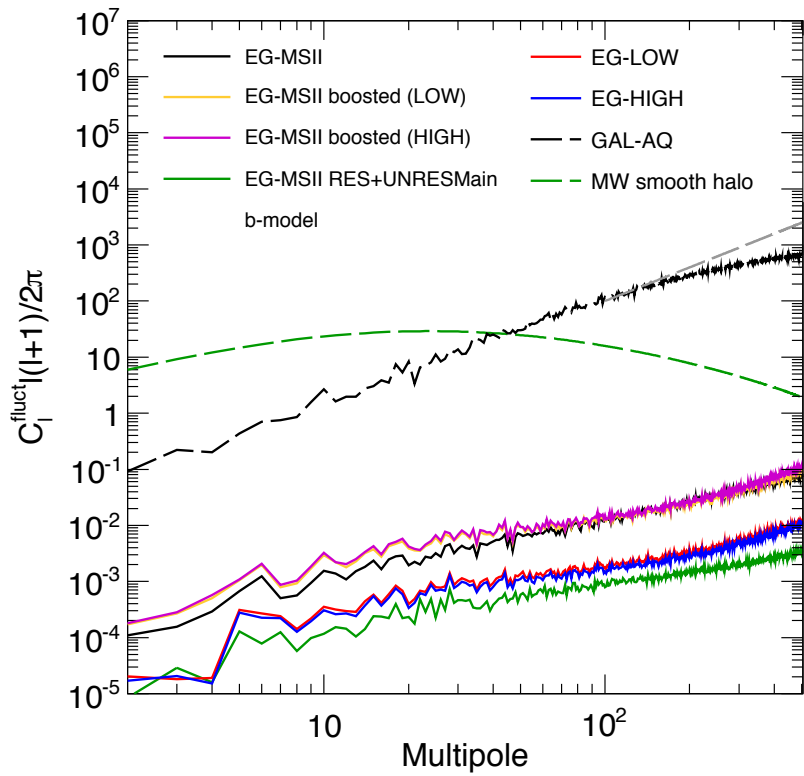
The angular power spectrum

$$I(\psi) = \sum_{\ell,m} a_{\ell m} Y_{\ell m}(\psi) \quad C_\ell = \langle |a_{\ell m}|^2 \rangle$$

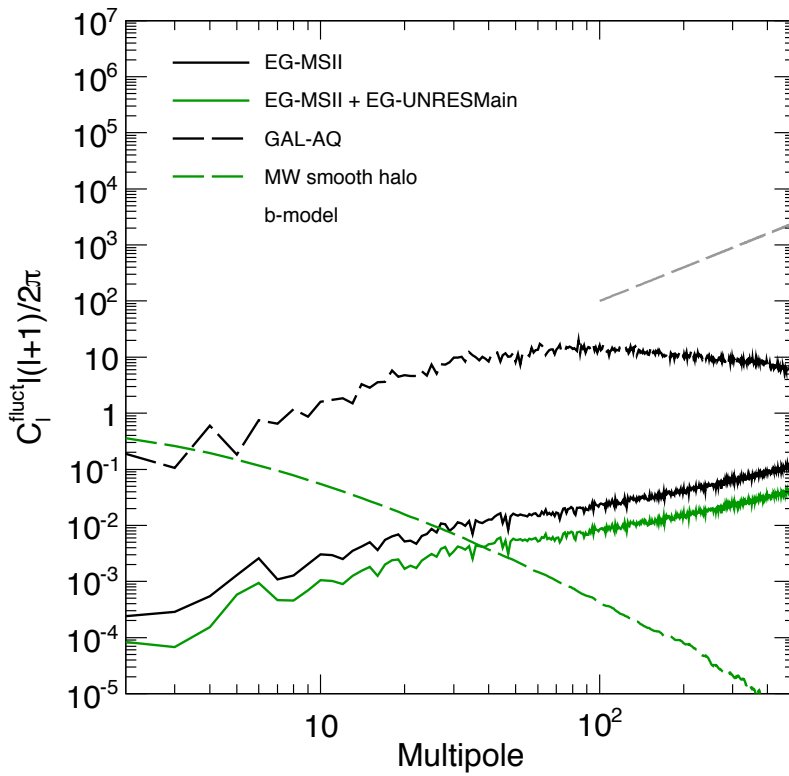
- intensity angular power spectrum: C_ℓ
 - indicates *dimensionful* amplitude of anisotropy
- fluctuation angular power spectrum: $\frac{C_\ell}{\langle I \rangle^2}$
 - *dimensionless*, independent of intensity normalization
 - amplitude for a single source class is the same in all energy bins (if all members have same energy spectrum)

Angular power spectra of dark matter signals

Predicted angular power spectrum of DM annihilation



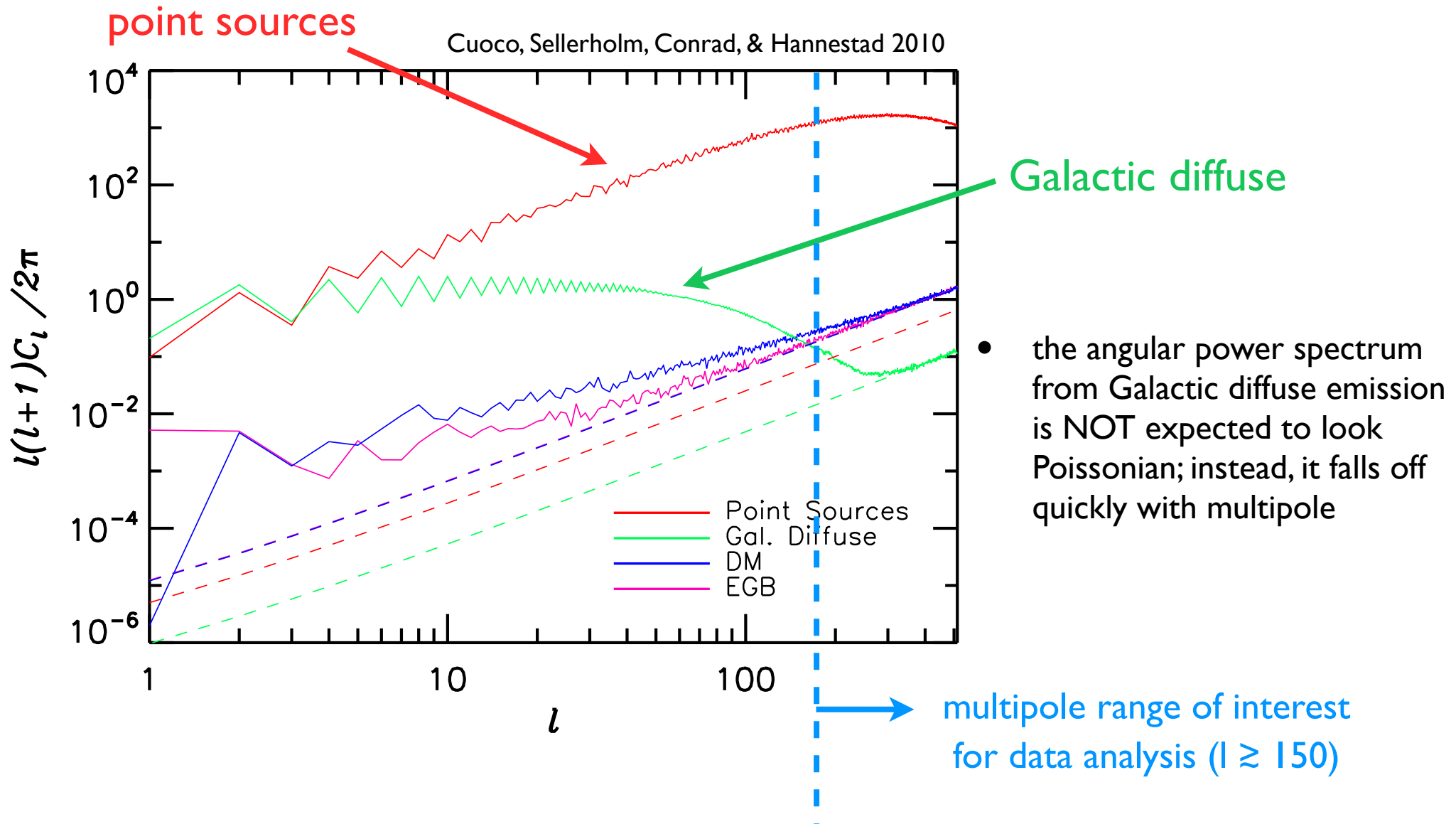
Predicted angular power spectrum of DM decay



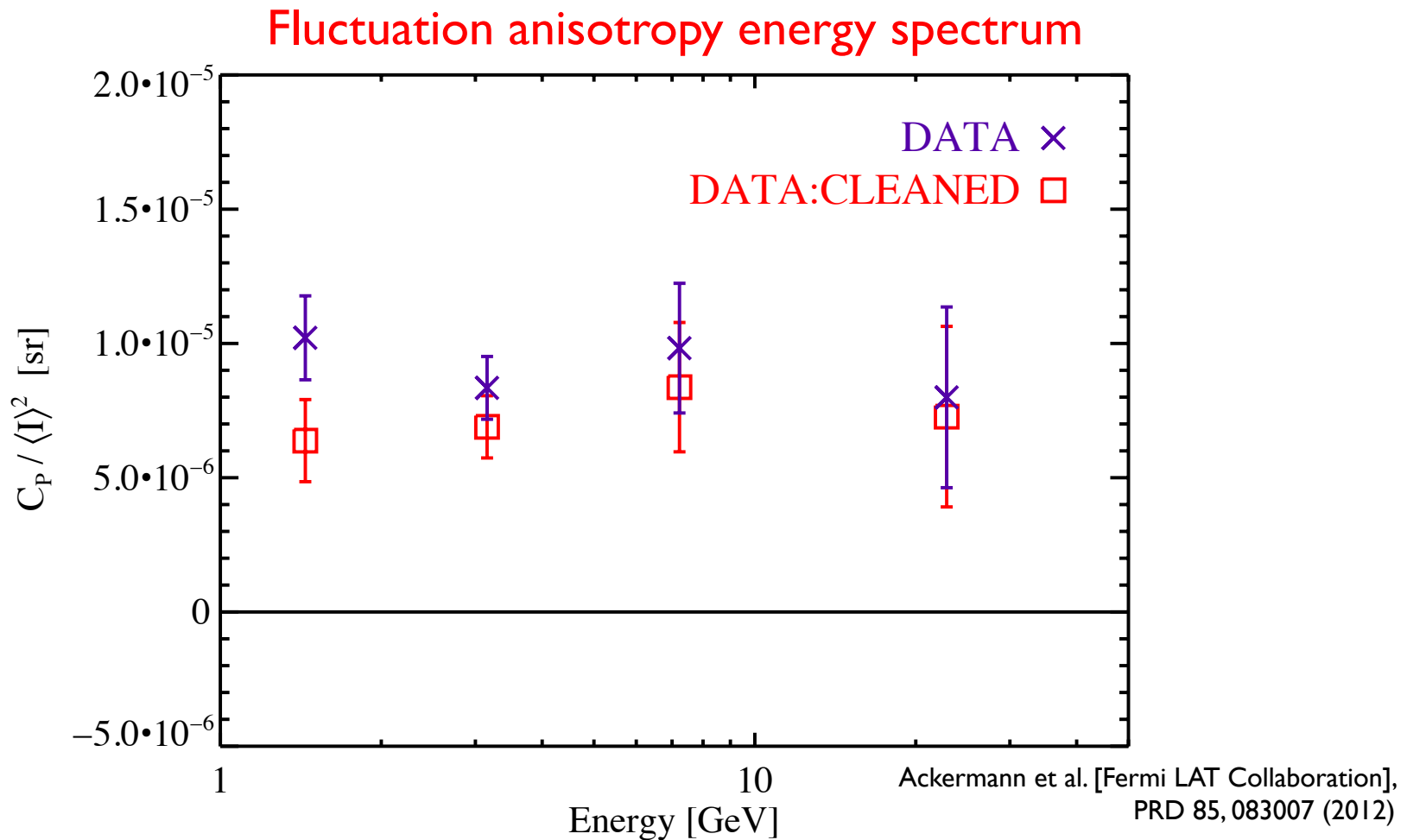
Fornasa, Zavala, Sanchez-Conde, JSG et al. 2012

- predictions derived from Millenium-II and Aquarius simulations and accurately account for redshifting and EBL attenuation for extragalactic DM, and secondary emission from Galactic DM
- the angular power spectrum of dark matter annihilation and decay falls off faster than Poisson at multipoles above ~ 100

Angular power spectra of foregrounds



Energy dependence of anisotropy



- consistent with no energy dependence, but mild or localized energy dependence not excluded
- consistent with all anisotropy contributed by one or more source classes contributing same fractional intensity at all energies considered

Source population constraints from anisotropy

- intensity angular power can constrain the absolute IGRB contribution from a single population

$$C_{P,i} \leq C_{P,\text{tot}}$$

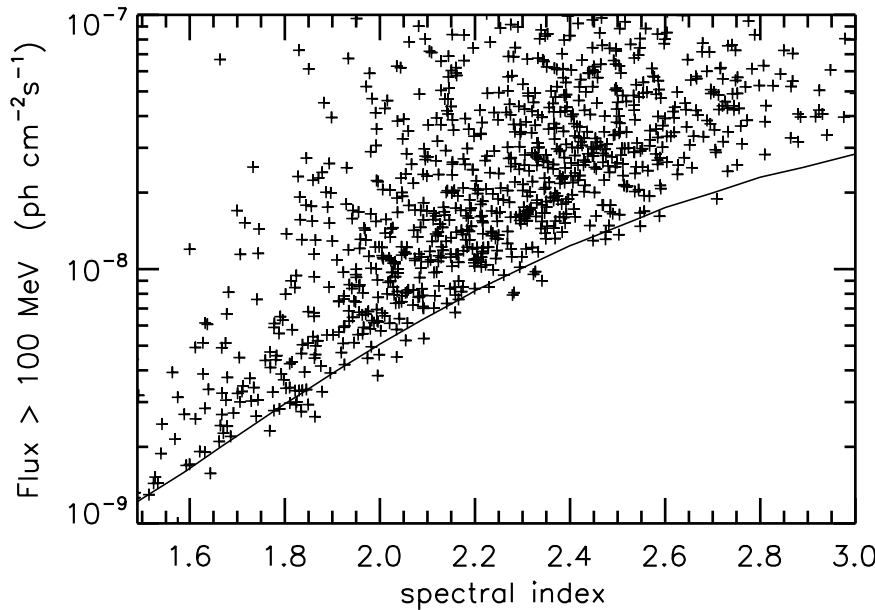
- fluctuation angular power can constrain the fractional IGRB contribution from a single population

$$f_i^2 \leq \frac{C_{P,\text{tot}} / \langle I_{\text{tot}} \rangle^2}{C_{P,i} / \langle I_i \rangle^2}$$

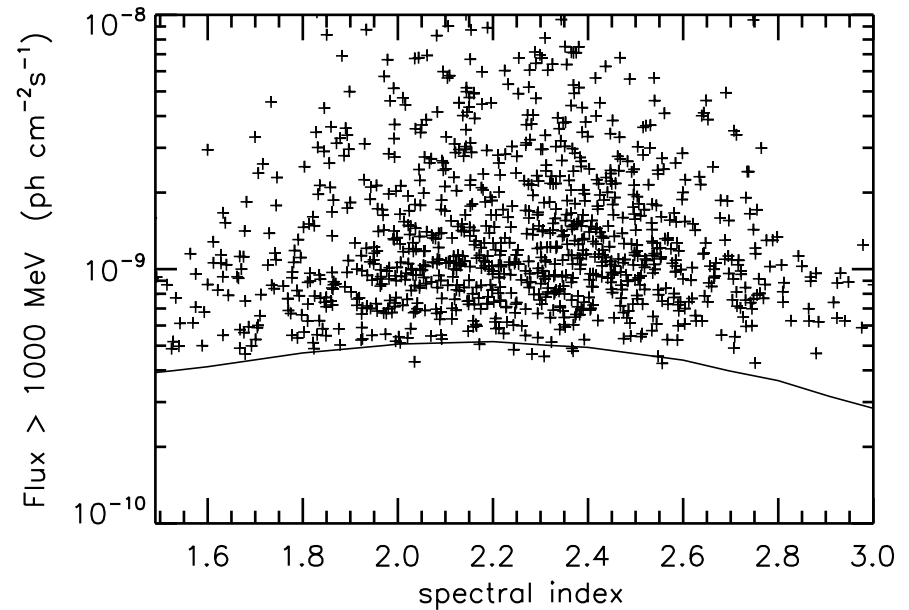
Aside: threshold fluxes and spectral index bias

In general, the source detection threshold can depend on the spectral index of the source (*spectral index bias*)

Source flux vs spectral index ($E > 100$ MeV)



Source flux vs spectral index ($E > 1$ GeV)



Cuoco, Komatsu & JSG 2012

(points are IFGL sources, lines are derived threshold flux as a function of spectral index)

spectral index bias is strong for fluxes > 100 MeV,
but small for fluxes > 1 GeV (1-10 GeV is used in this study)

Comparison with predicted angular power

Fluctuation angular power in data

$C_P / \langle I \rangle^2$ [10^{-6} sr]
10.2 ± 1.6
8.35 ± 1.17
9.83 ± 2.42
8.00 ± 3.37

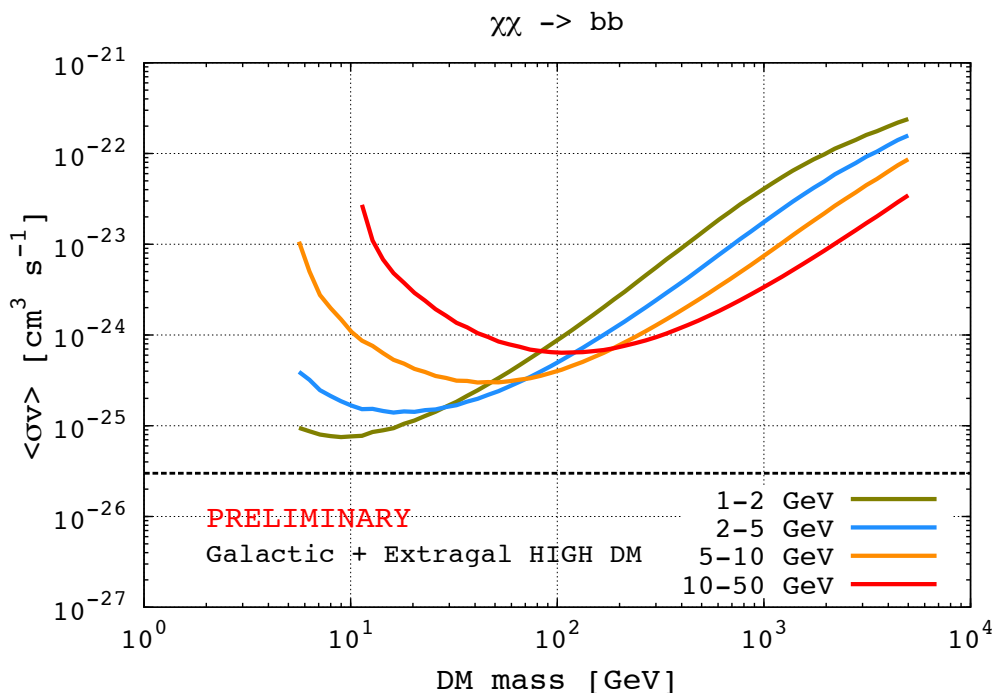
predicted fluctuation angular power $C_\ell / \langle I \rangle^2$ [sr] at $\ell = 100$ for a single source class
(LARGE UNCERTAINTIES):

- blazars: $\sim 2\text{e-}4$
- starforming galaxies: $\sim 2\text{e-}7$
- dark matter: $\sim 1\text{e-}6$ to $\sim 1\text{e-}4$
- MSPs: ~ 0.03

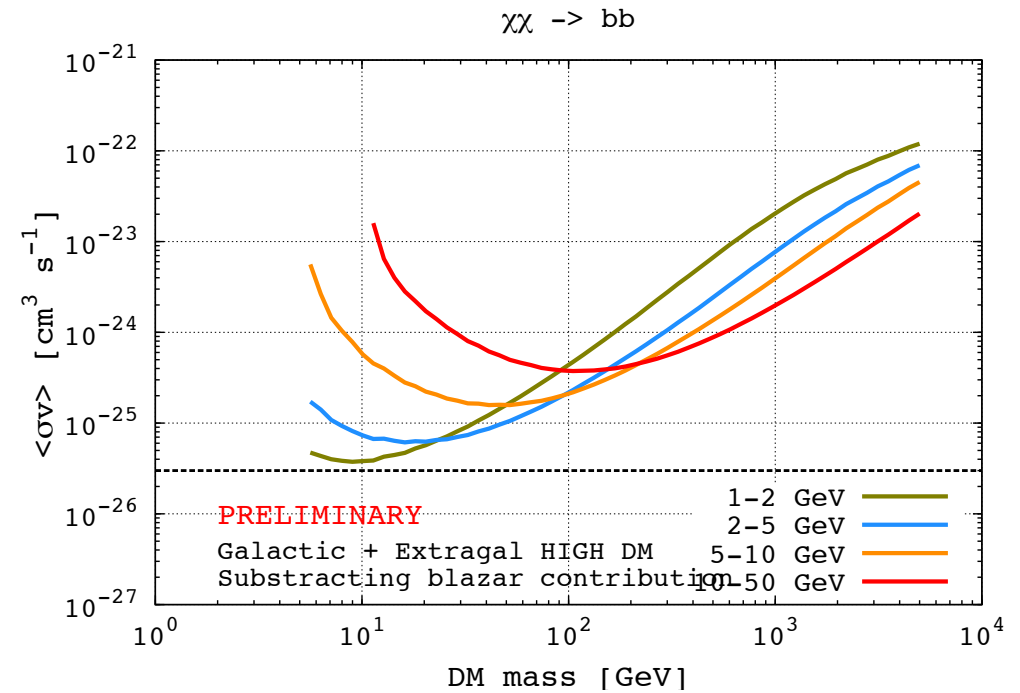
- fluctuation angular power of $\sim 1\text{e-}5$ sr falls in the range predicted for some astrophysical source classes and some dark matter scenarios
- can be used to constrain the IGRB contribution from these populations

Anisotropy constraints on dark matter models

Constraints using 2-sigma upper limit
on total measured anisotropy



Constraints using 2-sigma upper limits
on non-blazar anisotropy

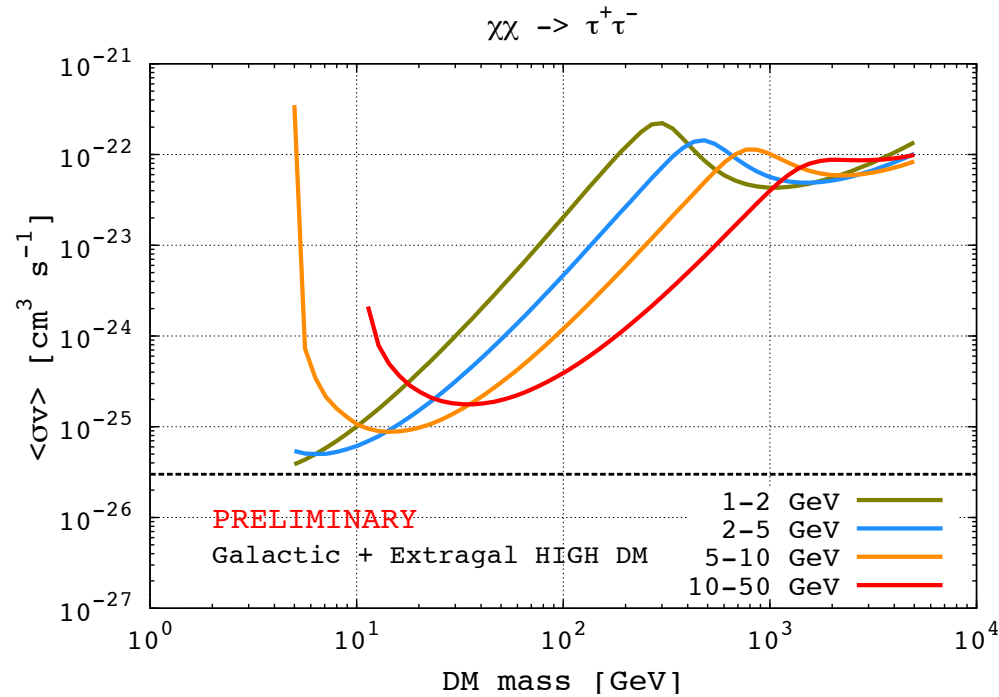


Fermi LAT collaboration and MultiDark, in prep

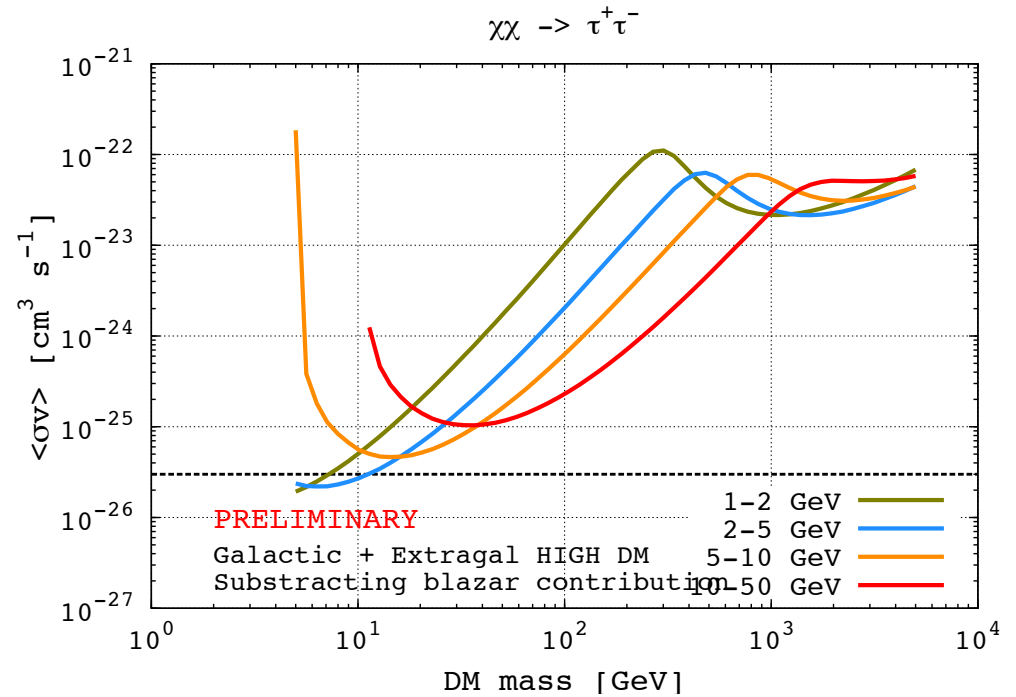
- preliminary dark matter constraints from published anisotropy measurement
- updated measurement should yield improved sensitivity due to more energy bins and improved statistics

Anisotropy constraints on dark matter models

Constraints using 2-sigma upper limit
on total measured anisotropy



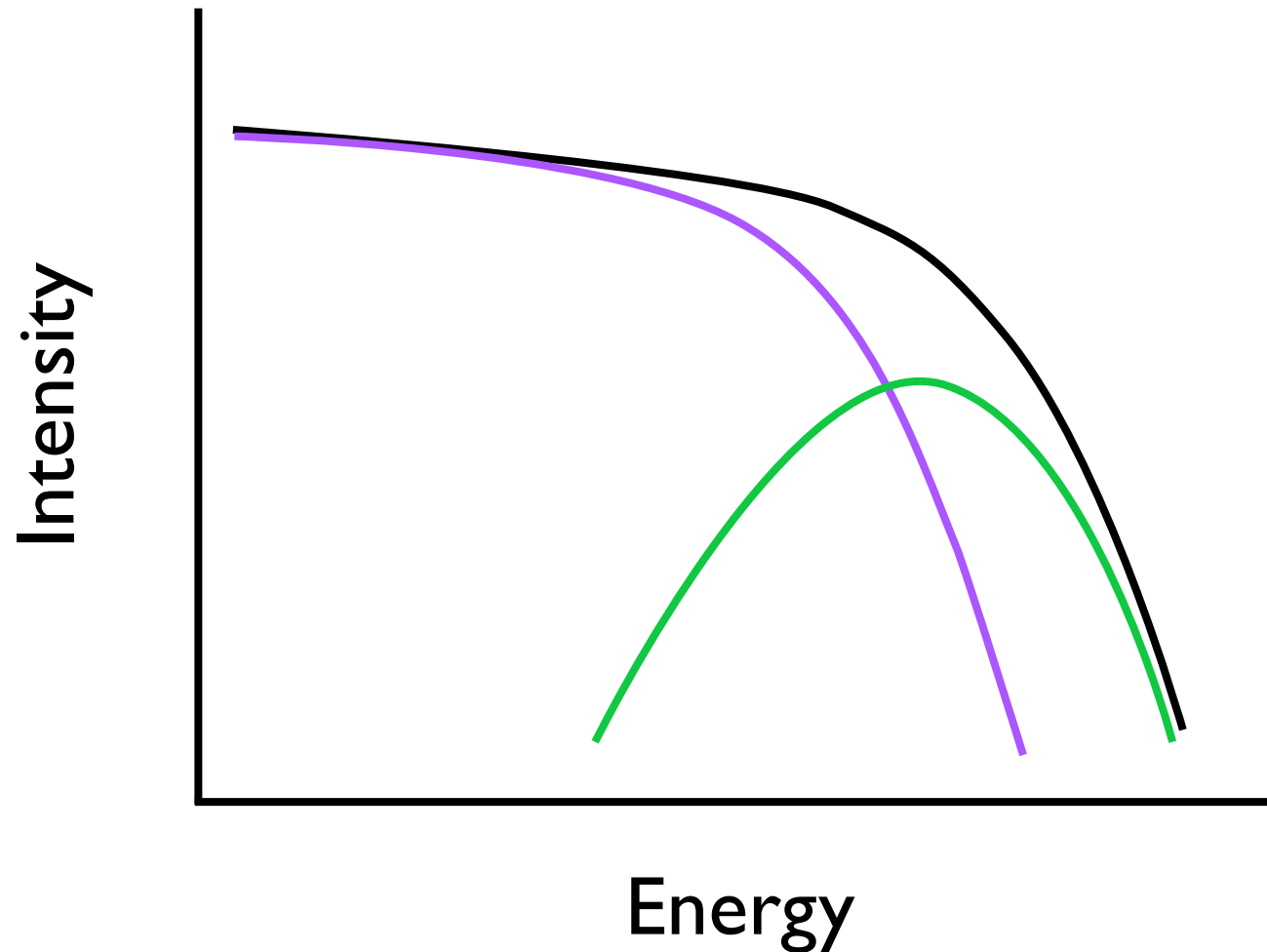
Constraints using 2-sigma upper limits
on non-blazar anisotropy



Fermi LAT collaboration and MultiDark, in prep

- preliminary constraints generated using published anisotropy measurement
- updated measurement should yield improved sensitivity due to more energy bins and improved statistics

Decomposing diffuse emission with anisotropy



Decomposing diffuse emission with anisotropy

assumptions:

- two-component scenario
- uncorrelated components
- each component defined by a single energy spectrum
- one component dominates the intensity at some energy

$$I_{\text{tot}}(E) = I_1(E) + I_2(E)$$

$$C_{\ell,\text{tot}}(E) = C_{\ell,1}(E) + C_{\ell,2}(E)$$

$$\hat{C}_{\ell,\text{tot}}(E) = \left(\frac{I_1(E)}{I_{\text{tot}}(E)} \right)^2 \hat{C}_{\ell,1} + \left(\frac{I_2(E)}{I_{\text{tot}}(E)} \right)^2 \hat{C}_{\ell,2}$$

Decomposing diffuse emission with anisotropy

assumptions:

- two-component scenario
- uncorrelated components
- each component defined by a single energy spectrum
- one component dominates the intensity at some energy

observables

$$I_{\text{tot}}(E) = I_1(E) + I_2(E)$$



$$C_{\ell,\text{tot}}(E) = C_{\ell,1}(E) + C_{\ell,2}(E)$$

$$\hat{C}_{\ell,\text{tot}}(E) = \left(\frac{I_1(E)}{I_{\text{tot}}(E)} \right)^2 \hat{C}_{\ell,1} + \left(\frac{I_2(E)}{I_{\text{tot}}(E)} \right)^2 \hat{C}_{\ell,2}$$

Decomposing diffuse emission with anisotropy

assumptions:

- two-component scenario
- uncorrelated components
- each component defined by a single energy spectrum
- one component dominates the intensity at some energy

observables

$$I_{\text{tot}}(E) = I_1(E) + I_2(E)$$

model parameters

$$C_{\ell,\text{tot}}(E) = C_{\ell,1}(E) + C_{\ell,2}(E)$$

$$\hat{C}_{\ell,\text{tot}}(E) = \left(\frac{I_1(E)}{I_{\text{tot}}(E)} \right)^2 \hat{C}_{\ell,1} + \left(\frac{I_2(E)}{I_{\text{tot}}(E)} \right)^2 \hat{C}_{\ell,2}$$

Decomposing diffuse emission with anisotropy

assumptions:

- two-component scenario
- uncorrelated components
- each component defined by a single energy spectrum
- one component dominates the intensity at some energy

observables

$$I_{\text{tot}}(E) = I_1(E) + I_2(E)$$

model parameters

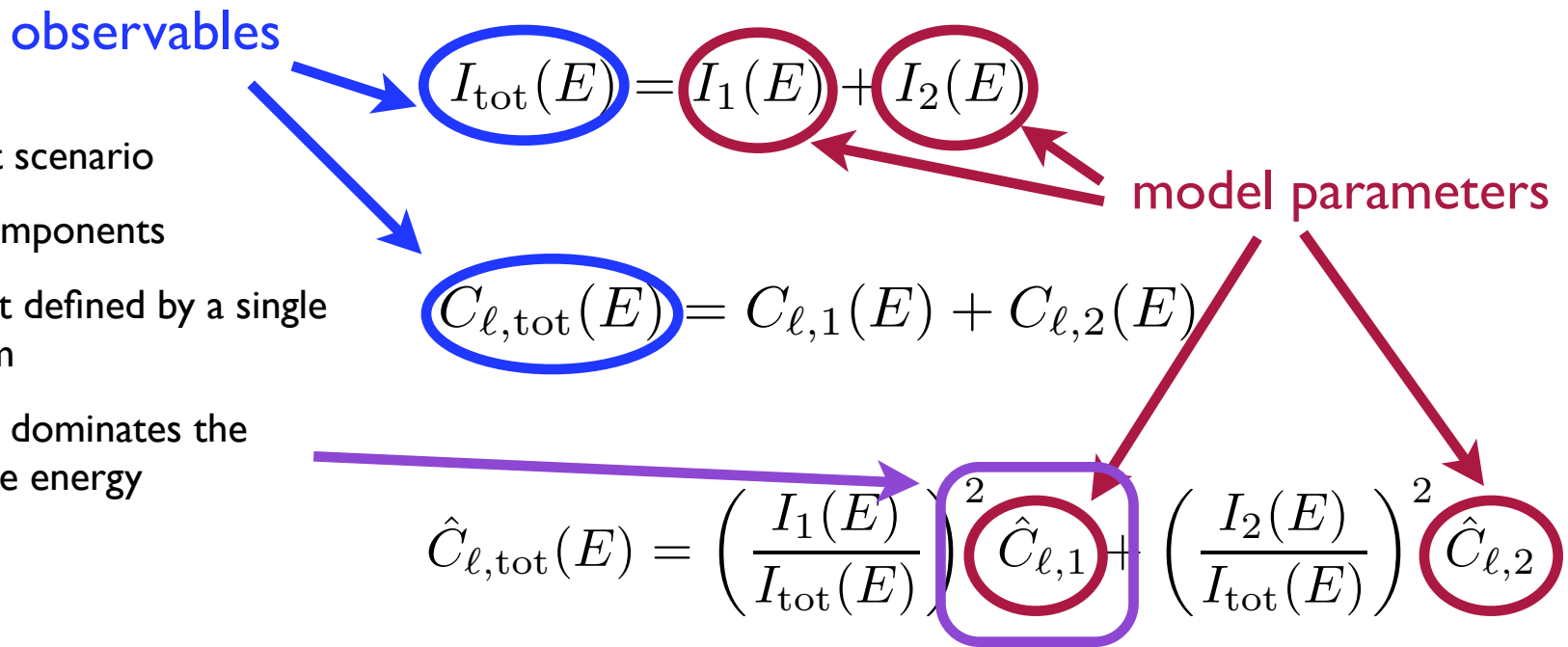
$$C_{\ell,\text{tot}}(E) = C_{\ell,1}(E) + C_{\ell,2}(E)$$

$$\hat{C}_{\ell,\text{tot}}(E) = \left(\frac{I_1(E)}{I_{\text{tot}}(E)} \right)^2 \hat{C}_{\ell,1} + \left(\frac{I_2(E)}{I_{\text{tot}}(E)} \right)^2 \hat{C}_{\ell,2}$$

Decomposing diffuse emission with anisotropy

assumptions:

- two-component scenario
- uncorrelated components
- each component defined by a single energy spectrum
- one component dominates the intensity at some energy



under these assumptions,

features observed in the anisotropy energy spectrum can be used
to extract each component's intensity spectrum

*without a priori assumptions about the shape of the intensity spectra
or anisotropy properties!*

The magic of algebra!

$$I_{\text{tot}}(E) = I_1(E) + I_2(E)$$

+

$$\hat{C}_{\ell,\text{tot}}(E) = \left(\frac{I_1(E)}{I_{\text{tot}}(E)} \right)^2 \hat{C}_{\ell,1} + \left(\frac{I_2(E)}{I_{\text{tot}}(E)} \right)^2 \hat{C}_{\ell,2}$$

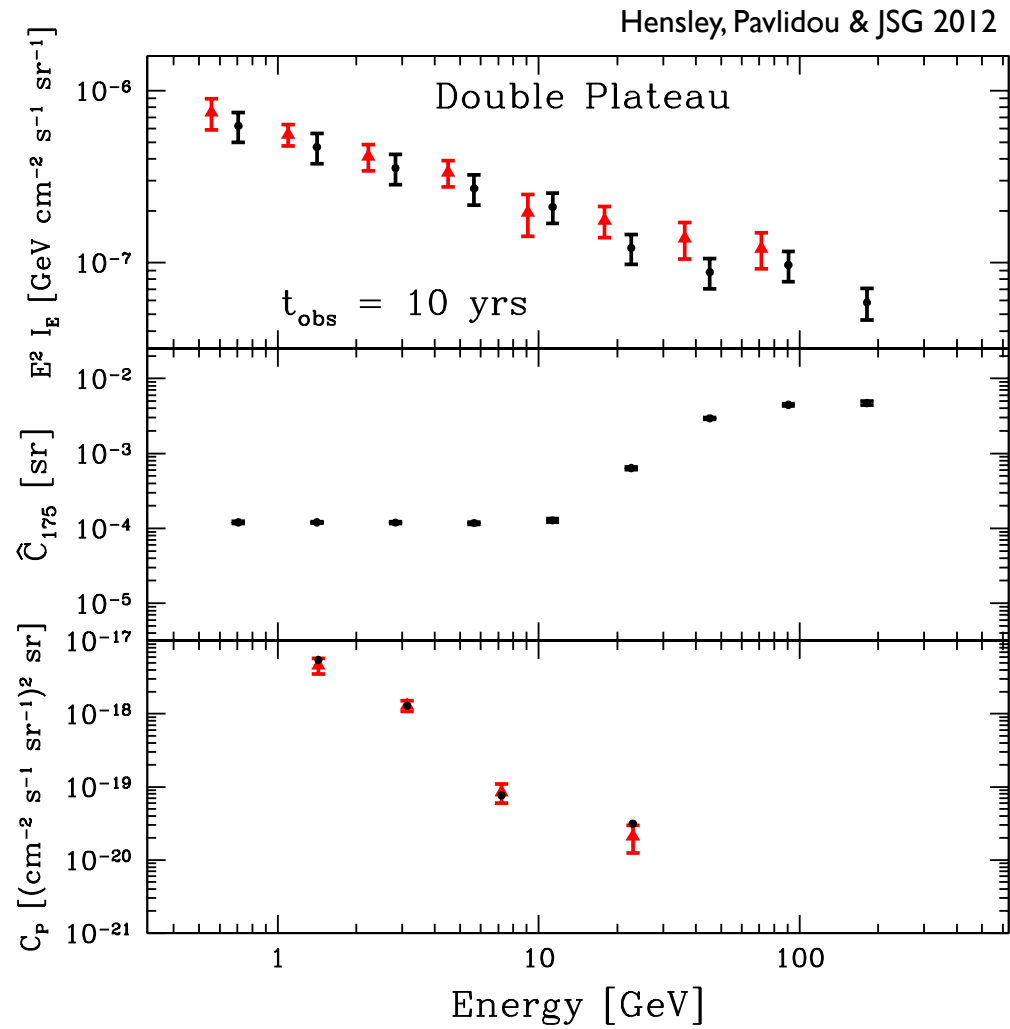


$$I_1 = I_{\text{tot}} \left(\frac{\hat{C}_{\ell,2} \pm \sqrt{\hat{C}_{\ell,1}\hat{C}_{\ell,\text{tot}} + \hat{C}_{\ell,2}\hat{C}_{\ell,\text{tot}} - \hat{C}_{\ell,1}\hat{C}_{\ell,2}}}{\hat{C}_{\ell,1} + \hat{C}_{\ell,2}} \right)$$

$$I_2 = I_{\text{tot}} \left(\frac{\hat{C}_{\ell,1} \mp \sqrt{\hat{C}_{\ell,1}\hat{C}_{\ell,\text{tot}} + \hat{C}_{\ell,2}\hat{C}_{\ell,\text{tot}} - \hat{C}_{\ell,1}\hat{C}_{\ell,2}}}{\hat{C}_{\ell,1} + \hat{C}_{\ell,2}} \right)$$

Example IGRB decomposition

Example observed intensity spectrum and anisotropy energy spectrum



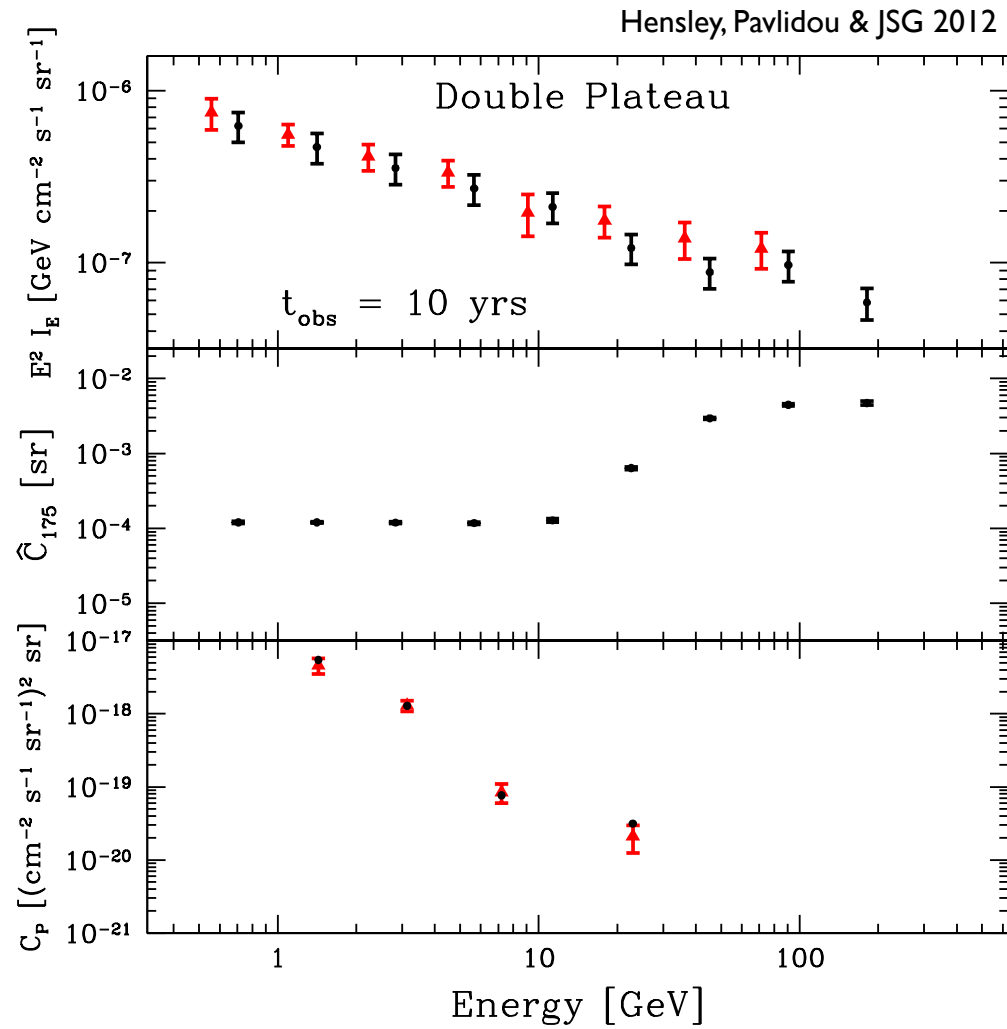
red = published LAT measurements

black = example scenario for 10 yrs LAT observations

- infer that one component dominates the intensity at the low plateau and one at the high plateau
- this yields the fluctuation anisotropy of each component; the intensity spectrum of each component can now be solved for

Example IGRB decomposition

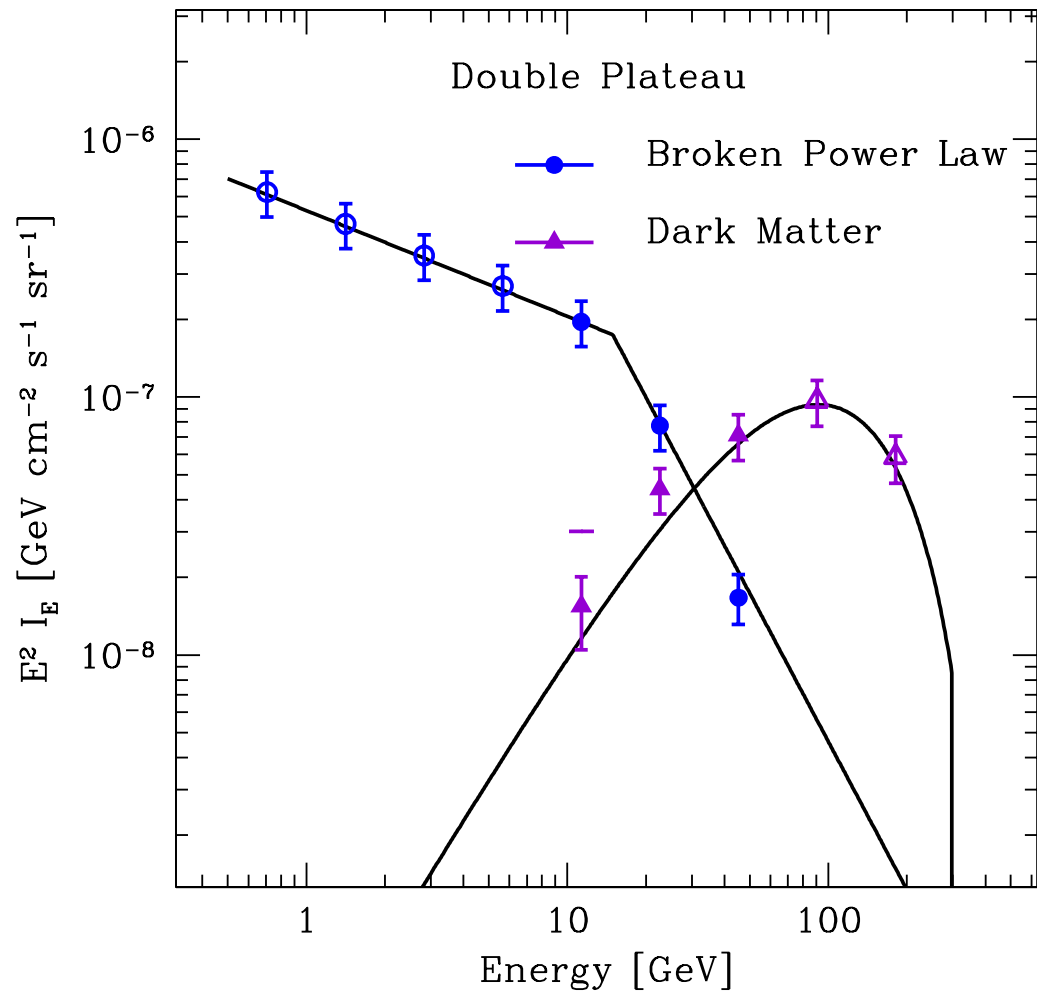
Example observed intensity spectrum and anisotropy energy spectrum



red = published LAT measurements

black = example scenario for 10 yrs LAT observations

Decomposed energy spectra



Separating signals with energy-dependent anisotropy

TABLE I: Summary of two-component decomposition techniques.

Method	Observational Signature	Inferred Properties of Components	Intensity Normalization Recovered?	Fluctuation Angular Power Recovered?
Double plateau	Plateaus at both high and low energies observed in anisotropy energy spectrum	One source dominant in anisotropy at low energies, other source dominant at high energies	Yes	Yes
Low-Anisotropy Plateau	Anisotropy energy spectrum rises from (falls to) a low-anisotropy plateau at low (high) energy	Source that is subdominant in intensity is much more anisotropic than the dominant source	No	No
High-Anisotropy Plateau	Anisotropy energy spectrum falls from (rises to) a high-anisotropy plateau at low (high) energy	Source that is subdominant in intensity is much less anisotropic than the dominant source	Yes	No
Known Zero-Anisotropy Component	None; requires <i>a priori</i> knowledge that one of the two components is isotropic	One source is completely isotropic	No	No
Minimum	Minimum observed in the anisotropy energy spectrum	Both source components have comparable intensity and anisotropy such that Eq. 20 is satisfied at some energy	Yes	Yes
Multiple- ℓ Measurements	Two distinct anisotropy energy spectra can be obtained at two different ℓ	\hat{C}_ℓ is a function of ℓ for at least one source such that two distinct anisotropy energy spectra can be obtained at different ℓ	Yes	Yes

Separating signals with energy-dependent anisotropy

TABLE I: Summary of two-component decomposition techniques.

Method	Observational Signature	Inferred Properties of Components	Intensity Normalization Recovered?	Fluctuation Angular Power Recovered?
Double plateau	Plateaus at both high and low energies observed in anisotropy energy spectrum	One source dominant in anisotropy at low energies, other source dominant at high energies	Yes	Yes
Low-Anisotropy Plateau	Anisotropy energy spectrum rises from (falls to) a low-anisotropy plateau at low (high) energy	Source that is subdominant in intensity is much more anisotropic than the dominant source	No	No
High-Anisotropy Plateau	Anisotropy energy spectrum falls from (rises to) a high-anisotropy plateau at low (high) energy	Source that is subdominant in intensity is much less anisotropic than the dominant source	Yes	No
Known Zero-Anisotropy Component	None; requires <i>a priori</i> knowledge that one of the two components is isotropic	One source is completely isotropic	No	No
Minimum	Minimum observed in the anisotropy energy spectrum	Both source components have comparable intensity and anisotropy such that Eq. 20 is satisfied at some energy	Yes	Yes
Multiple- ℓ Measurements	Two distinct anisotropy energy spectra can be obtained at two different ℓ	\hat{C}_ℓ is a function of ℓ for at least one source such that two distinct anisotropy energy spectra can be obtained at different ℓ	Yes	Yes

Constraints from the IGRB

